

## Cooperation of membrane-translocated syntaxin4 and basement membrane for dynamic mammary epithelial morphogenesis

Yuina Hirose<sup>1</sup> and Yohei Hirai<sup>1,2\*</sup>

1; Department of Biomedical Chemistry, Graduate School of Science and Technology, Kwansai Gakuin University. 2-1, Gakuen, Sanda 669-1337, Japan

2; Department of Biomedical Sciences, Graduate School of Biological and environmental Sciences, Kwansai Gakuin University. 2-1, Gakuen, Sanda 669-1337, Japan

\*; Corresponding

Tel: +81-79-565-7234

E-mail: y-hirai@kwansai.ac.jp

### Keywords

mammary gland, syntaxin4, epithelial morphogenesis, epimorphin, basement membrane, epithelial-mesenchymal transition

### Summary statement

We identified a novel regulatory element for epithelial morphogenesis: a t-SNARE protein extruded by the lactogenic hormone and basement membrane components coordinately lead to mammary cyst formation.

### Abstract

Mammary epithelia undergo dramatic morphogenesis after puberty. During pregnancy, luminal epithelial cells in ductal trees are arranged to form well-polarized cystic structures surrounded by a myoepithelial cell layer, an active supplier of the basement membrane (BM). Here, we identified a novel regulatory mechanism in this process by using a reconstituted BM-based three-dimensional culture and aggregates of a model cell line EpH4, which had been manipulated for inducible expression of a t-SNARE protein syntaxin4, either in an intact or signal peptide-connected form, and

those genetically deficient in syntaxin4. We found that cells extruded syntaxin4 upon stimulation with the lactogenic hormone, prolactin, which in turn accelerated the turnover of E-cadherin. In response to extracellular expression of syntaxin4, cell populations that were less affected by BM actively migrated and integrated into the BM-faced cell layer. Concurrently, the BM-faced cells, which were simultaneously stimulated with syntaxin4 and BM, acquired unique epithelial characteristics to undergo dramatic cellular arrangement for cyst formation. These results highlight the importance of the concerted action of extracellular syntaxin4 extruded by the lactogenic hormone and BM components in epithelial morphogenesis.

## Introduction

Epithelial morphogenesis is an important biological process for building tissue-specific epithelial architectures, where epithelial cells are assembled into three-dimensional (3D) structures composed of well-polarized epithelial sheets, in which cells are tightly connected by several junctional apparatuses. In this process, an array of systemic signaling factors and extracellular matrix proteins coordinately and spatiotemporally regulate intercellular junctional components connected to cytoskeletons, creating mechanical forces to produce a 3D configuration of the epithelial cell sheets (Friedl and Mayor, 2017; Roignot et al., 2013). While active epithelial morphogenesis occurs in several tissues during embryogenesis, this process is accompanied by cellular differentiation and is substantially irreversible. In contrast, the postnatal mammary gland is very unique: fully differentiated epithelial cells undergo morphogenesis, which is accompanied by their prominent cellular arrangement under the strict control of lactogenic hormones (Macias and Hinck, 2012; Paine and Lewis, 2017). Thus, gestation-induced morphological changes in the mammary epithelia are considered one of the most relevant models that provide a molecular basis for epithelial morphogenesis (Ivanova et al., 2021; Shamir and Ewald, 2015).

In the pubertal mammary gland, luminal epithelial cells form single-layered tubes in primary ducts and side branches, the tips of which are often occupied by piled-up cells. In the virgin glands, they also exist as stratified aggregates at the end of elongating ducts termed terminal end buds (TEBs). Upon stimulation with lactogenic hormones, however, they undergo a dramatic cellular arrangement to actively form lobular structures comprising well-polarized cysts called acini or alveoli (Briskin and O'Malley, 2010; Macias and Hinck, 2012; Sternlicht et al., 2006). During this morphogenic

process, all the luminal epithelial cells in the ducts and the outermost cells in the stratified ductal tips are surrounded by myoepithelial cells that actively produce major basement membrane (BM) components (Gudjonsson et al., 2005; Paine and Lewis, 2017). Moreover, these luminal cells are often in direct contact with BM components that lie outside the myoepithelial cell layer (Vidi et al., 2013). Focusing on the characteristics of lumen formation, three compelling mechanisms have been proposed: 1) apoptotic elimination of certain cell populations (Martín-Belmonte et al., 2008), referred to as the cavitation model (Debnath and Brugge, 2005); 2) expansion of apical cargo trafficking sites between cells as a result of coordinated cell division and polarization (Bryant et al., 2010); and 3) fusion of microlumens by hydraulic fracturing of cell-cell contact (Dumortier et al., 2019). Recently, Neumann et al. clearly showed that apoptosis is not involved in mammary lumen formation (Neumann et al., 2018); however, a causal cue for the hormone-dependent quick cellular arrangement, as well as its regulatory mechanism in the mammary epithelia remains elusive.

From a mechanistic point of view, the spatial epithelial-mesenchymal transition (EMT) accompanied by a reduction in polarity and intercellular adhesion in certain cell populations, has been suggested to be a leading cause of collective cell migration (Campbell and Casanova, 2016; Ewald et al., 2012). So far, the plausible regulators of the local EMT process include insoluble BM components; their impacts on the cells vary depending on the position in the tissue (Ewald et al., 2012). Indeed, epithelial cells are known to exhibit anchorage-dependent behaviors (Martín-Belmonte et al., 2008), and those adhering directly to the BM exhibit profound epithelial characteristics, such as enhanced cell-cell adhesion, decreased motility, and stronger polarity (Bryant et al., 2014; Chen et al., 2013). In fact, cells situated within the TEB, inside of which are substantially free from the effects of BM, frequently show reduced intercellular adhesion, thereby potentially rearranging and exchanging their positions even in the absence of hormonal stimuli (Ewald et al., 2008; Ewald et al., 2012; Hinck and Silberstein, 2005).

E-cadherin, an abundantly expressed intercellular adhesion molecule in mammary epithelia, is a key element responsible for the arrangement and maintenance of organized epithelial structures throughout their developmental stages. It is well known that functional ablation or downregulation of this molecule is accompanied by EMT-like cell behavior, and vice versa (Lamouille et al., 2014). In addition, E-cadherin-mediated adhesion often influences signaling pathways and regulates several genes involved in cell survival and proliferation (Shamir and Ewald, 2015). E-cadherin interacts with actin filaments or microtubules via catenins, its cytoplasmic binding partner, or via a certain

member of the calmodulin-regulated spectrin-associated proteins (CAMSAPs) (Meng et al., 2008; Takeichi, 2014). While a number of studies have identified molecular elements that hamper E-cadherin-mediated intercellular adhesion, most of them target cytoplasmic junctions between E-cadherin and epithelial cytoskeletons (Fukata et al., 1999; Kuroda et al., 1998). We recently reported a direct interaction between the extracellular domain of E-cadherin and certain members of plasmalemmal syntaxins at the cell surface, which severely affected E-cadherin functions (Hirose et al., 2018).

Syntaxins are t-SNARE proteins that mediate intravesicular fusion in the cytoplasm. Among syntaxins, syntaxin2 (epimorphin) and syntaxin4 temporally translocate across the cell membrane in response to external stimuli and subsequently execute their latent morphogenic and differentiation-inducing functions in several cell types (Hagiwara-Chatani et al., 2017; Kadono et al., 2015; Okugawa and Hirai, 2008; Radisky et al., 2009). Given that their extracellular exposure occurs without the requirement of a time-consuming transcription and translation process, the effect of their morphogenic actions is thought to be very quick and sensitive. Using a mammary epithelial cell line, SCp2, we showed that certain cell populations extruded syntaxin4 upon stimulation with the lactogenic hormone, prolactin, which in turn perturbed E-cadherin function and propagated EMT-like signals. Consistently, the local presence of extracellular syntaxin4 in Scp2 aggregates led to asymmetric tissue organization in the collagen gel (Hirose et al., 2018). In contrast, another study using the same cells cultured on plastic showed that the effect of syntaxin4 was possibly deregulated by an insoluble BM component, laminin, as a consequence of the direct intermolecular interactions between them (Shirai et al., 2017).

In the present study, we analyzed the functional relationship between prolactin-provoked extracellular syntaxin4 and BM components in the spatial cellular arrangement of mammary epithelial cells, and revealed that the spatiotemporal coordination of extruded syntaxin4 and BM components could play a key role in mammary epithelial morphogenesis.

## **Results**

### Expression of syntaxin4 in the mammary gland

Luminal epithelial cells in mammary glands undergo stage-specific morphogenesis under hormonal control. For example, those in the pubertal period gradually transform into elongating ducts with side branches, the tips of which often exhibit stratified structures. In young animals, the tips of the

elongating ductal tree exhibit unique structures called terminal end buds (TEBs) that function as a platform for subsequent morphogenesis. In contrast, those after a gestational period are actively rearranged to build up lobular structures, comprising of single-layered epithelial cysts surrounded by a myoepithelial cell layer, which gradually inflates and exhibits clear apicobasal polarity for milk secretion. Syntaxin4 was detected in all the cellular compartments regardless of the developmental stage, including luminal epithelial, myoepithelial, fibroblastic and adipocytic cells. At the tip of a side branch in the pubertal gland (at 7 weeks of age), all multilayered luminal epithelial cells can express syntaxin4 at the cell membrane in an apolar fashion. In contrast, single-layered luminal epithelial cells in the acini/alveoli of a lactating gland can express this molecule at the basolateral membrane (Fig. 1A). Immunostaining of luminal epithelial cells cultured with the lactogenic hormone prolactin, reveals membrane translocation and extracellular expression of syntaxin4 in a certain cell population (Fig. 1A).

Prolactin provokes membrane translocation of syntaxin4, which instructs dynamic cellular arrangements

Given that the non-tumorigenic murine mammary epithelial cell line, EpH4, reportedly retains hormonal responses, morphogenic potential, and clear apical-basal polarity, we next tested whether these cells also extruded endogenous syntaxin4 under lactogenic conditions. As observed in the primary cells, the extracellular expression of syntaxin4 upon treatment with prolactin is obvious in some EpH4 cells (Fig. 1B), suggesting that EpH4 can provide a useful cell model system to define the role of syntaxin4. We next investigated possible changes in three-dimensional (3D) cell behaviors depending on the amount of extracellular syntaxin4 provoked by prolactin. To this end, we generated EpH4 cells deficient in syntaxin4 (Stx4 K.O. EpH4) and those with inducible expression of syntaxin4 with T7 tag (T7-Stx4 EpH4) (Fig. 1C). These cells were then aggregated as previously described (Hirai et al., 1998) and cultured in reconstituted BM matrix Matrigel, given that myoepithelial cells enveloping luminal epithelial cells *in vivo* actively produce BM components. In conventional hormone-free medium, aggregates of these EpH4 derivatives, either deficient in syntaxin4 or inducible expression of exogenous syntaxin4 does not exhibit any discernible phenotypes (Fig. 1C). In contrast, in the medium containing prolactin, T7-Stx4 EpH4 cell aggregates, regardless of the expression of exogenous syntaxin4, undergo a dramatic cellular arrangement to form multiple lumens inside, somewhat similar to lobular-alveolar development during

pregnancy/lactation. While apicobasal polarity is not clearly established in these cells, such a meaningful cell behavior is not observed in syntaxin4-deficient Stx4 K.O EpH4 cells and is more prominent in T7-Stx4 EpH4 cells with exogenous syntaxin4 (Fig. 1C). To determine whether syntaxin4 impacts fundamental cell behavior, we compared the shapes of Stx4 K.O EpH4 cells to that of parental EpH4 cells in two-dimensional (2D) culture. Treatment with prolactin led to flattened morphology in EpH4 cells, and r-F3, a membrane-impermeable recombinant fragment of syntaxin4 (Glu198-Lys272) which has acted as a potent antagonist of extracellular syntaxin4 (Hirose et al., 2018), substantially attenuating this effect. In contrast, morphology of Stx4 K.O EpH4 cells was never affected by prolactin nor r-F3, implicating that the effects of prolactin are attributed, at least in part, to extracellularly extruded syntaxin4 (Fig. S1). However, we could not test the effect of this antagonistic fragment in 3D culture, since this fragment is rapidly trapped by laminin in Matrigel (Shirai et al., 2017) and would not be accessible to the cells.

#### Induction of clear cystic structure by extracellularly presented syntaxin4

To clarify the effect of extracellular syntaxin4, we generated EpH4 cells with inducible expression of T7-tagged syntaxin4 fused with a signal peptide for extracellular translocation (Sig-T7-Stx4). Upon induction of syntaxin4 on the surface of the entire cells, Sig-T7-Stx4 cell aggregates underwent dramatic cellular arrangement to form cystic structures with a large central lumen, even in the absence of prolactin (Fig. 2A, B). While the cellular arrangement is so dramatic that the additive effects of prolactin in these cells was not appreciable, the phenotypic appearance (exhibiting multiple or single lumen) is clearly dependent upon the mode (partial or total cells) of extracellular expression of syntaxin4 (Fig. 1C, 2A and S2). These results highlight the role of extracellularly extruded syntaxin4 on epithelial morphogenesis in the mammary gland. The overall cystic structure of Sig-T7-Stx4 in Matrigel is similar to that of the acini/alveoli in the pregnant/lactating mammary glands (Fig. 2C). Transmission electron microscopy analyses reveal that these cysts are composed of single-layered epithelial sheets with representative intercellular junctional complexes, including desmosomes and tight junctions (TJs) (Fig. 2D, E). In addition, the well-developed microvilli of cells in the cystic structure were exposed only toward the luminal spaces with an accumulation of a TJ component, zonula occludens-1 (ZO-1), at the lumen-proximal region, suggesting that these cells acquired apicobasal polarity (Fig. 2D, E). According to the 3D images, the basal surface of the cysts appeared smooth (Fig. 2E). In contrast, in the absence of induction of extracellular syntaxin4, these

cells are alive but remain in tightly packed cell clumps (Fig. 2D, E). These results demonstrate that extracellularly presented syntaxin4 contributes to the reorganization of cell aggregates into cystic structures with apicobasal polarity in Matrigel, which is reminiscent of the epithelial compartment in the mammary acini/alveoli.

#### Syntaxin4-induced morphogenesis is independent to cell growth and apoptosis

While the size of syntaxin4-induced cysts continues to increase for several days, there are no significant differences in the total number of cells, regardless of induction by extracellular syntaxin4, as judged by the amount of  $\beta$ -actin (Fig. 3A and B). This is not the case when the same experiments were performed using another epithelial cell line MDCK II, which reportedly exhibits clear polarity and possesses the ability to form cystic structures in Matrigel, even in the absence of hormonal stimuli and exogenous transgenes. While the sizes of MDCK II cell aggregates are practically unchanged during culture, each formed a luminal space within a few days (Fig. 3C). Given that the production of lumen in MDCK II involves apoptotic elimination of Matrigel-free central cells in the aggregates (Martín-Belmonte et al., 2008), those in EpH4 with extracellular syntaxin4 might be independent of apoptotic cell death. As expected, the active form of effector caspase (caspase 3) was detectable in the luminal side of MDCKII cysts, but not in the syntaxin4-induced ones (Fig. 3D), and the formation/expansion of the latter was not hindered by the functional ablation of caspases with ZVAD-FMK (Fig. 3E).

#### EpH4 cells improve locomotive ability in response to extracellular syntaxin4

Next, we addressed successive cellular migratory behaviors in the aggregates in response to extracellular syntaxin4. Time-lapse imaging revealed that the inner cells in the aggregates do not succumb to apoptosis but actively migrate (Fig. 4A, and Movie 1). In the 2D culture, these cells with morphological changes dissociate from colonies and migrate outward upon induction of extracellular syntaxin4 (Fig. 4B), implying an onset of epithelial-mesenchymal transition (EMT). Among all keratin genes tested (11 keratins in total), six keratins exhibit significant changes in their expression (more than 1.5-fold change) in response to extracellular syntaxin4, while five appear to be downregulated. In addition, eight MMP genes out of 13 show significant changes, and the top three, including *MMP9*, appear to be clearly upregulated (Fig. 4C and D).

### Behaviors of Matrigel-faced EpH4 cells expressing extracellular syntaxin4

The cell behaviors observed are quite different when they are directly attached to Matrigel; changes in mobility and intercellular adhesiveness by extracellular syntaxin4 are visibly attenuated in the 2D culture (Fig. 5A). In addition, the confluent cell sheet on Matrigel displaying sustained expression of extracellular syntaxin4 often forms dome-like structures with clear intercellular junctions (Fig. 5B). We have previously shown that the C-terminal globular domain of laminin, a major BM component, and glycosaminoglycan (GAG) side chains of a laminin receptor interact with extracellular syntaxin4 so as to potentially counteract its function (Shirai et al., 2017). However, RNA sequencing analyses reveal that changes in the expression of EMT markers affected by extracellular syntaxin4 (Fig. 4C, D) are not restored in cells stimulated simultaneously with Matrigel. While some keratin genes are prone to reactivation, the augmented expression of the MMPs remains constant or further upregulated (Fig. 5C). In addition, a number of molecular elements involved in intercellular adhesions and those in epithelial polarity are dramatically upregulated in response to simultaneous stimulation with both extracellular syntaxin4 and Matrigel (Fig. 5D), suggesting that extracellular syntaxin4 and BM components do not simply antagonize each other or propagate individual signals independently, but cooperatively elicit unique responses in the epithelial cells (Fig. 5C and D). Furthermore, we also found that EpH4 cells situated away from Matrigel could smoothly integrate into the confluent cell sheet on Matrigel if they expressed extracellular syntaxin4 (Fig. 5E). Such syntaxin4-triggered distinct regulatory effects depending on the influence of Matrigel might account for the multicellular arrangement, that is, in response to extracellular syntaxin4 cells that are less affected by BM actively move to and smoothly integrate into the polarized cell layer facing the BM, and this layer acquires unique epithelial characteristics to undergo dramatic cellular arrangements for the formation and expansion of cystic structures. Consistently, when cell aggregates are embedded in collagen gel, the outermost cell population is radially scattered, instead of contributing to luminal morphogenesis (Fig. S3).

### Extracellular syntaxin4 triggers turnover of E-cadherin

We then addressed the effect of syntaxin4-dependent dysregulation on cell-cell adhesion systems in the absence of the BM effect. Previously, we showed that extracellular syntaxin4 directly binds to E-cadherin, a critical player in epithelial cell-cell adhesion (Hirose et al., 2018), to hinder its intrinsic cell adhesive function without affecting its mRNA expression. The direct association between the



central and membrane proximal domains of syntaxin4 and E-cadherin extracted from EpH4 cells is ascertained again (Fig. S4). We can observe a significant reduction in the intact form of syntaxin4 in cells after treatment with prolactin, which is partly prevented by chloroquine (an inhibitor of the protein-elimination system in lysosomes), in a dose-dependent manner (Fig. 6A, B). Intriguingly, extracellular expression followed by lysosomal degradation of extracellular syntaxin4 appears to be coincident with the appearance and lysosomal degradation of a 90 kDa form of E-cadherin protein (Fig. 6B). To further clarify whether the extracellular but not the intracellular form of syntaxin4 is responsible for these phenomena, we compared the effects of intact syntaxin4 and its signal peptide-connected form in the absence of prolactin but in the presence of chloroquine. We found that the dose-dependent effects of chloroquine were reproduced only for the extracellular form of syntaxin4, demonstrating that extracellularly present syntaxin4 readily undergoes lysosomal degradation along with the 90 kDa E-cadherin (Fig. 6C, D). Based on the assumption that a direct interaction between syntaxin4 and E-cadherin at the cell surface initiates the elimination process, we analyzed the expression pattern and physical characteristics of these proteins in cells treated with chloroquine. A subpopulation of syntaxin4 and E-cadherin is co-assembled to converge on the same dot-like structures in the cytoplasm, although their original expression was at the cell surface, exhibiting insoluble characteristics (Fig. 6E, F, S5A). Regarding this 90 kDa form of truncated E-cadherin, polyclonal antibodies against its cytoplasmic domains fail to recognize this form (Fig. S5B), and its amount is clearly decreased by the proteasome inhibitor, lactacystin (Fig. 6G), suggesting that the shift in the molecular size of E-cadherin (124-90 kDa) is ascribed to the proteasomal processing of its cytoplasmic tail. However, despite the fact that E-cadherin is processed, internalized, and degraded in cells with extracellular syntaxin4, the amount of the functional 124 kDa form is unaltered (Fig. 6D). Together with the observation that mRNA expression of E-cadherin is not affected by extracellular syntaxin4 also in this cell system (Fig. S5C), these results suggest a dramatic increase in E-cadherin turnover with intermittent exposure of “tailless” E-cadherin in cells with extracellular syntaxin4. Interestingly, the syntaxin4-induced turnover of E-cadherin remains in cells facing the Matrigel (Fig. S5D), confirming that signals by extracellular syntaxin4 and BM components do not simply antagonize each other.

### Syntaxin4-dependent E-cadherin turnover and role of Matrigel in a simple cell system

To further define the biological significance of extracellular syntaxin4 on E-cadherin turnover with intermittent exposure of tailless E-cadherin and concerted action with BM components, we conducted experiments using fibroblastic L cells, which have no intrinsic cell adhesion molecules and are much less responsive to BM components (Kiener et al., 2009; Nagafuchi et al., 1987). These cells with stable expression of the full-length E-cadherin transgene (designated as EL cells) exhibit cell-adhesive properties caused solely by E-cadherin (Nagafuchi et al., 1987). Notably, however, only the expression of the E-cadherin transgene is enough to exhibit strong cell-adhesive properties in L cells (Nagafuchi et al., 1994), EL cells do not lose features of fibroblasts (Chen and Obrink, 1991), suggesting that L cells endogenously possess or can rapidly form catenin/actin complex for the cytoskeletal linkage of E-cadherins. We found that EL cells additionally introduced with the “tailless” form of E-cadherin appear to retain cell-cell adhesion in 2D, but gradually weaken the E-cadherin-mediated cell-cell adhesion without affecting the amount of functional full-length E-cadherin (Fig. S6). Based on these observations, we generated EL cells with inducible expression of extracellular syntaxin4 and used them for biological validation. Upon induction of extracellular syntaxin4, the amount and insolubility of syntaxin4 and 90 kDa E-cadherin appear to increase in the presence of chloroquine, indicating the acceleration in E-cadherin turnover occurs also in this cell system (Fig. 7A, B). While the instantaneous activity of E-cadherin is practically unchanged by the extracellular expression of syntaxin4 (Fig. S7), cells in syntaxin4-expressing EL cell aggregates gradually weaken the cell-cell contact in 3D and the outermost cells are scattered with exposing filopodial protrusions (Fig. 7C), confirming the extracellular role of syntaxin4 as a functional repressor of E-cadherin.

Altogether, a novel and plausible mechanism underlying dynamic cellular arrangements for epithelial morphogenesis is demonstrated in this study, which could explain how mammary epithelial cells build the alveolar structure during pregnancy. Hormones actively secreted during the gestational period trigger temporal translocation of syntaxin4 across the membrane, and extracellularly extruded syntaxin4 exerts distinct morphogenic functions depending on the cellular context modulated by BM signals. That is, extracellular syntaxin4 affects cell populations that are less affected by BM-producing myoepithelial cells to migrate and integrate into the cell layer facing to BM/myoepithelial cells, while this molecule propagates unique signals to the cell populations faced by BM/myoepithelial cells for the construction of cystic structures (Fig. 8).

## Discussion

### Membrane translocation of syntaxin4

We first demonstrated that the lactogenic hormone prolactin induced membrane translocation of the t-SNARE protein syntaxin4 in EpH4 cells, as observed in the cultured lactogenic mammary epithelial cells. While this could be a key event for the subsequent cellular arrangement, the machinery for extracellular extrusion of syntaxin4 is completely unknown to date. However, that of epimorphin, a cognate membrane-tethered syntaxin, may provide referential information, such as calcium influx, leading to extracellular extrusion of a multi-protein complex containing epimorphin and phosphatidylserine-bound annexin II from cells (Hirai et al., 2007). Prolactin has been reported consistently increase calcium uptake in the cytoplasm (Bolander, 1985), and annexin II is involved in prolactin-induced milk secretion (Burgoyne et al., 1991; Zhang et al., 2018). Alternatively, stimulated mammary epithelial cells that are capable of secreting intracytoplasmic lipids containing phosphatidylserine (Smoczyński, 2017) are thought to export syntaxin4 extracellularly together with milk fat globules.

### Extracellular syntaxin4 increases cellular motility and accelerates E-cadherin turnover

Once presented extracellularly, syntaxin4 cooperated with BM components to trigger a dramatic arrangement in cells. While a previous study suggested the possible contribution of apoptosis to mammary luminal morphogenesis (Debnath et al., 2002), a recent report demonstrated that this process could proceed without the requirement of cell demise (Akhtar and Streuli, 2013; Neumann et al., 2018). In line with these observations, we demonstrated that syntaxin4-induced mammary cyst formation proceeds solely by spatiotemporal changes in epithelial cell adhesion, mobility, and polarity. Notably, extracellularly exposed syntaxin4 elicited the onset of EMT-like cell responses if the cells were free from the effects of BM. This raises the question as to how syntaxin4 confers locomotive ability in these cells. To this end, we showed that syntaxin4 extruded extracellularly became accessible and directly bound to the major intercellular adhesion molecule, E-cadherin, via its central and membrane-proximal domains, which could be a cue for the degradation of E-cadherin. Experiments using inhibitors of protein elimination systems showed that the cytoplasmic domain of E-cadherin is degraded by the proteasome upon being associated with syntaxin4 in the extracellular environment, which gives rise to the production of a 90 kDa form that lacks a cytoplasmic tail for

cytoskeletal linkage. The protein complex containing the “tailless” form of E-cadherin and syntaxin4 was then rapidly internalized, delivered to lysosomes, and displayed highly insoluble characteristics, after which it was ultimately eliminated. Dysfunctional E-cadherin is known to be ubiquitinated in the juxtamembrane domain and degraded by the proteasome and subsequently by lysosomes (Sako-Kubota et al., 2014). In addition, internalization of E-cadherin in EpH4 cells upon EMT has been shown to be mediated by clathrin-coated vesicles, which are retrievable only from the highly insoluble fraction (Janda et al., 2006). Given that E-cadherin homeostasis is regulated by the small GTPase Cdc42, which is indispensable for alveolar development in mammary glands (Druso et al., 2016; Georgiou et al., 2008; Leibfried et al., 2008), elucidation of its relationship with extracellular syntaxin4 is an important issue that needs to be addressed in future research. While the rapid elimination of “tailless” E-cadherin with unaltered mRNA expression was obvious in cells with syntaxin4, the amount of functional full-length E-cadherin appeared to be constantly maintained, implying that translation of this adhesion molecule is augmented by syntaxin4. Although further experiments using syntaxin4-transfected cells and translation inhibitors were not feasible since the expression of the syntaxin4-transgene is also repressed, we found that E-cadherin protein, but not of its mRNA, was dramatically decreased by extracellular syntaxin4 in some other cell types (Hagiwara-Chatani et al., 2017; Hagiwara et al., 2013), indicating that E-cadherin translation is facilitated only in certain cell types. Nevertheless, the constant expression and active elimination of E-cadherin suggest its active turnover and intermittent disruption by the E-cadherin-mediated intercellular adhesion system.

#### Cooperation between extracellular syntaxin4 and BM components

E-cadherin, as a main intercellular adhesion molecule, is linked to the cytoskeleton, and its turnover has been shown to severely affect the collective migration of epithelia (Brüser and Bogdan, 2017; Kota et al., 2019; Kowalczyk and Nanes, 2012; Song et al., 2013; Takeichi, 2014). Temporal reduction in epithelial identity, including loss of polarity and increased cell motility, has been reported in inner cell populations in stratified epithelia during active morphogenesis (Ewald et al., 2012). In contrast, E-cadherin dynamics are not the sole determinant of locomotive behavior in these cells. Actually, the effect of the forced expression of “tailless” E-cadherin was relatively weak in EL cells compared to EpH4 cells, where both cells similarly express functional full-length E-cadherin, but changes in the cellular context (expression of EMT-related markers, for example)

were more prominent in EpH4 cells (data not shown). In addition, although active turnover of E-cadherin also occurred in syntaxin4-expressing EpH4 cells adherent to reconstituted BM Matrigel, EMT-like cell behaviors were not observed even in the presence of extracellular syntaxin4. Instead, they were tightly connected to each other with a well-developed intercellular junctional apparatus and displayed apicobasal polarity. Furthermore, cells cultured on Matrigel often form enclosed, single-layered, dome-like structures if they express extracellular syntaxin4. RNA sequencing analyses revealed that these cells acquired unique epithelial characteristics for the formation of enclosed and well-polarized cysts. On the other hand, the cell populations that were less affected by BM might actively migrate in response to extracellular syntaxin4 and smoothly integrate into BM-faced cell layers, thus participating in the production of cystic structures. This functional coordination model by extracellular syntaxin4 provoked by prolactin and BM components clearly rationalizes the spatial cellular dynamics and plasticity observed in prolactin-triggered luminal morphogenesis in mammary epithelia *in vivo*. We consistently detected a significant difference in the locomotive behaviors of the same cells with extracellular syntaxin4 in collagen gels, and of syntaxin4-expressing EL cells that were less responsive to laminin. The outermost cell populations in both the cases dissociated and radially scattered in the 3D substrates.

#### Extracellular extrusion of and possible role of plasmalemmal syntaxins

We have previously shown that extracellularly extruded epimorphin exerts a function similar to that of syntaxin4, in terms of induction of luminal morphogenesis (Bascom et al., 2005; Hirai, 2001; Hirai et al., 1992; Lehnert et al., 2001). While epimorphin is produced in mammary myoepithelial cells and secreted extracellularly upon proteolytic cleavage at the juxtamembrane site, it is substantially under-expressed in luminal epithelial cells (Bascom et al., 2005; Hirai et al., 1998). In contrast, syntaxin4 is ubiquitously and abundantly detectable in a wide variety of epithelial cell types (Bennett et al., 1993; Ding et al., 2018) and lacks a cleavage site for secretion (Hirai et al., 2007). Although this protein undoubtedly exists on the cytoplasmic surface of the plasma membrane as a t-SNARE protein and temporally forms unique protein complexes with certain cytoplasmic components for intravesicular fusion (Duan et al., 2020), it would be interesting to investigate whether a subpopulation of syntaxin4 is extruded extracellularly upon external stimuli in these tissues, to exert its latent morphogenic functions. If this is the case, extracellular syntaxin4 might be a critical morphogenic regulator or at least contribute to the development of well-polarized epithelial

architectures. To date, the extracellular extrusion with limited secretion of syntaxin4 (Kadono et al., 2012) and its involvement in tissue morphogenesis/cell differentiation is evident in the skin epidermis and embryonic stem cells (Hagiwara-Chatani et al., 2017; Hagiwara et al., 2013; Kadono et al., 2015). Attempts to identify signals and molecular elements involved in the membrane translocation of syntaxin4 in the respective tissues are now underway.

## Materials & methods

### Mice and mammary glands

Mammary glands were collected from ICR or BALB/C mice (7 weeks of age, pregnancy period day 13, and lactation period day 1) purchased from SLC (Shizuoka, Japan). For whole-mount staining, the glands were fixed with Methacarn solution and stained with Carmine Alum solution (Stem Cell Technologies, Vancouver, Canada), as previously described (Murata et al., 2015). Some glands were fixed with methanol at -20°C, cryosectioned, and analyzed by immunohistochemistry. All experiments using mice were approved by the Committee for Animal Experimentation at Kwansei Gakuin University (approval number: 2020-27)

### Cells and transfectants

The mouse mammary luminal epithelial cell line EpH4 (Fialka et al., 1996), Madin-Darby canine kidney cell line MDCK II (CRL2936 from ATCC), and mouse fibroblast cell line L and its derivative EL (Nagafuchi et al., 1987) were maintained in DMEM/Ham's F12 medium (Wako, Japan) supplemented with 10% fetal bovine serum (FBS), penicillin and streptomycin (DH10). Cells with a tetracycline-repressive expression system were maintained in DH10 supplemented with 5 µg/mL tetracycline (tet). To generate cells with tet-regulated T7-tagged syntaxin4, or T7-tagged syntaxin4 containing an N-terminal fusion of an exogenous signal peptide from *IL-2*, cDNA encoding the corresponding polypeptide (Hagiwara-Chatani et al., 2017) was subcloned into a PiggyBac-based tet-regulatable expression plasmid (Woltjen et al., 2009). EpH4 cells and EL cells were stably transfected with the generated plasmid together with pTet-TAK (Thermo Fisher Scientific, St. Louis, USA), pCAG-PBase, and pSV40Neo using Lipofectamine 2000 (Invitrogen, St. Louis, USA). After G418 selection, cell clones expressing exogenous syntaxin4 upon removal of tetracycline were isolated and expanded. To knockout the syntaxin4 gene in EpH4 cells, the CRISPER/Cas9 system was used. EpH4 cells were transfected with pSpCas9 BB-2A-Puro plasmid

(Addgene, Mass., USA) in which one of the annealed DNAs (target-1: positive strand, 5'-CACCGCGACAGGACCCACGAGTTG-3'; negative strand, 5'-AAACCAACTCGTGGGTCCTGTCGC-3'; target-2: positive strand, 5'-CACCGTGGGTCCTGTCGCGCATGG-3'; negative strand, 5'-AAACCCATGCGCGGACAGGACCCAC-3') has been inserted into Bbs I restricted sites, selected using puromycin-containing DH10, cloned, and tested for complete ablation of syntaxin4 expression. As the sequence of target-2 contained 5'-UTR, cells generated by this target (clone 2) could re-express this molecule by introduction with the syntaxin4 expression cassette containing only the syntaxin4-coding region.

#### Reagents for cell treatment

Prolactin was purchased from Sigma-Aldrich and added to some cultures at a concentration of 3 µg/mL, along with 1 µg/mL hydrocortisone (Wako, Tokyo), which reportedly improved the genetic potential (Mills and Topper, 1970). Chloroquine, an inhibitor of lysosome degradation (Sigma-Aldrich, St. Louis, USA) was dissolved in PBS and used at concentrations of 50 or 100 µM. A pan-caspase inhibitor, ZVAD-FMK (Selleck, Tokyo, Japan) and a selective proteasome inhibitor, lactacystin (Abcam, Cambridge, UK) were dissolved in DMSO and used at a concentration of 20 µM and 10 µM, respectively.

#### Three-dimensional culture

Cells ( $2.0 \times 10^5$ / 500 µL) were seeded in each well of a 24-well plate, the bottom of which was pre-coated with 1% agarose gel, and rotated at 100 rpm for 24 h at 37 °C, resulting in the formation of well-rounded cell aggregates, as previously described (Hirai et al., 1998). The cell aggregates were then collected, suspended in ice-cold Matrigel (Corning, NY, USA), seeded in 96-well plates, and incubated at 37 °C. After gelation, DH10 medium with (syntaxin4 OFF) or without (syntaxin4 ON) tetracycline was added to each well.

#### Transcriptional analysis

Total RNA was extracted using a Total RNA Extraction Miniprep System (VIOGENE, USA) and reverse-transcribed with an RNA-PCR kit (Takara, Shiga, Japan). Quantitative real-time PCR (qRT-PCR) was performed using Fast Start Essential DNA Green Master on a Light Cycler Nano system (Roche, Basel, Switzerland). The cDNAs were amplified using primer pairs for matrix metalloproteinase-3 (*MMP-3*) (5'-TGCAGCTCTACTTTGTTCTTTGA-3' and

5'-AGAGATTTGCGCCAAAAGTG-3') and *MMP-9* (5'-AGACGACATAGACGGCATCC-3' and 5'-TCGGCTGTGGTTCAGTTGT-3'). The relative expression of mRNA was normalized to that of *GAPDH*. To determine the transcriptional profiles of cells with and without syntaxin4, and on collagen and Matrigel, total RNA was extracted as described above, and RNA-sequencing analysis was outsourced to Macrogen Japan Corp. (Tokyo, Japan) for the comprehensive data source, which successfully processed data on 13,095 genes. To analyze the molecular elements of EMT-like cell behaviors, all keratins and MMPs that exhibited substantial changes compared to the comparative group (more than 1.5-fold) in the word categories “keratin (11 genes)” and “MMP (13 genes)” were extracted and listed. To analyze the molecular elements regulated by synergistic effects by syntaxin4 and Matrigel, all genes exhibiting substantial changes in the word categories “cell-cell adhesion” and “apical/basal part of the cells” between syntaxin4-expressing cells (Sig-Stx4 ON) cultured on Matrigel and collagen control were listed (65 genes from the former, and 31 genes from the latter). The six (for cell-cell adhesion) or seven (for apical/basal part of the cells) genes at the top of the list showing the largest changes downward were extracted and further analyzed in cells without syntaxin4 (Sig-Stx4 OFF) but with Matrigel.

#### Immunodetection

Antibodies used for the experiments included those against  $\beta$ -actin (A3854 from Sigma-Aldrich, St. Louis, USA) at 1:5000 dilution, alpha-tubulin (T9026 from Sigma-Aldrich, St. Louis, USA) at 1:1000 dilution, T7-tag (PM022 from MBL Life Science, Tokyo, Japan) at 1:1000 dilution, and caspase-3 (9664S from Cell Signaling Technology, MA., USA) at 1:1000 dilution. Monoclonal antibodies against E-cadherin and ZO-1 were gifted by Dr. Takeichi and Dr. Nagafuchi, respectively. Immunoblot analysis was performed according to standard procedures, and immunohistochemistry and immunocytochemistry were performed using the following protocol. Cell aggregates were fixed with 4% paraformaldehyde (PFA) in Tris-buffered saline (TBS) for 1 h and permeabilized with 0.5% Triton X-100 for 30 min. Cells cultured on dishes were fixed with 4% PFA in TBS for 10 min and permeabilized with 0.1% Triton X-100 for 10 min. Each sample was then incubated with 5% FBS for 1 h, primary antibody overnight, and labeled with secondary antibodies for 2 h, followed by extensive washing with TBS at each interval. Nuclei were counterstained with DAPI (Sigma-Aldrich, St. Louis, USA). Samples were mounted on glass slides and analyzed using an A1 confocal microscope system (Nikon, Tokyo, Japan) or Leica TCS SPE (Leica, Wetzlar, Germany).



#### Detection of proteins expressed at the cell surface

To detect extracellularly expressed proteins in EpH4 cells, living cells cultured in Transwell chambers (1.0  $\mu\text{m}$  in diameter, Costar, N.Y., U.S.) were washed with PBS and treated with 0.1 mg/mL Sulfo-NHS-SS biotin (Thermo Fisher Scientific, MA, USA) in PBS from both apical (0.5 mL) and basal (1 mL) sides for 30 min. After washing with DH10 several times to inactivate the NHS group in the residual NHS-SS-biotin, cells were lysed in lysis buffer (1% Triton-X100 and 1% NP-40 in TBS). Biotinylated cell surface proteins were then retrieved with NeutrAvidin beads (Thermo Fisher Scientific, MA, USA) and analyzed by immunoblotting.

#### Cell fraction insolubilized in cell lysis buffer

Cells treated with lysis buffer were centrifuged at 13,000 rpm for 15 min, and the resultant supernatant and pellet were treated as the soluble and insoluble fractions, respectively.

#### Time-lapse imaging

Cell migratory behavior in the aggregates was analyzed by recording microscopic images in every 60 min for 5 days using a Cellwatcher (Corefront, Tokyo, Japan). Time-lapse movies were obtained from the recorded images.

#### Ultrastructural analyses

To determine the ultrastructural characteristics of cysts induced by extracellular syntaxin4, the cultured samples with and without tetracycline were treated with 2% glutaraldehyde in PBS. These samples were sent to the Hanaichi Ultrastructure Research Institute (Aichi, Japan) to obtain transmission electron microscopy images.

#### Dissociation assay for instantaneous cell-cell adhesion mediated by E-cadherin

To know the instantaneous cell adhesive property in EL cells, we conducted the dissociation assay according to an established protocol (Nagafuchi et al., 1994). EL cells that have been introduced with tet-regulatable expression plasmid for extracellular syntaxin4 were pre-cultured for three days with or without tetracycline. These cells were then treated with 0.01% trypsin for 20 minutes in HEPES-buffered saline containing 2 mM  $\text{CaCl}_2$ , dissociated through 10 times pipettings, and number of dissociated single cells and size of the undissociated cell aggregates were analyzed. Parental L cells were used as a control.

Statistical analyses

Results are expressed as the mean  $\pm$  SD from at least three independent experiments. Data were analyzed by a Student's t-test and a p-value of  $< 0.05$  was considered statistically significant.

## Acknowledgements

We thank Drs. Takeichi and Nagafuchi for EL cells and antibodies against E-cadherin (ECCD2) and ZO-1. We are grateful to all members of Hirai laboratory for helpful discussions.

## Competing interests

No competing interests declared

## Funding

Part of this work was supported by Grant-in Aid for Scientific Research (19J22142 to Yu H., 17K09739 to Yo. H.), KG Special Research Fund (167AB0177a to Yo.H.)

## References

**Akhtar, N. and Streuli, C. H.** (2013). An integrin-ILK-microtubule network orients cell polarity and lumen formation in glandular epithelium. *Nat Cell Biol* **15**, 17-27.

**Bascom, J. L., Fata, J. E., Hirai, Y., Sternlicht, M. D. and Bissell, M. J.** (2005). Epimorphin overexpression in the mouse mammary gland promotes alveolar hyperplasia and mammary adenocarcinoma. *Cancer Res* **65**, 8617-21.

**Bennett, M. K., Garcia-Ararras, J. E., Elferink, L. A., Peterson, K., Fleming, A. M., Hazuka, C. D. and Scheller, R. H.** (1993). The syntaxin family of vesicular transport receptors. *Cell* **74**, 863-73.

**Bolander, F. F., Jr.** (1985). Possible roles of calcium and calmodulin in mammary gland differentiation in vitro. *J Endocrinol* **104**, 29-34.

**Brüser, L. and Bogdan, S.** (2017). Adherens Junctions on the Move-Membrane Trafficking of E-Cadherin. *Cold Spring Harb Perspect Biol* **9**.

**Briskin, C. and O'Malley, B.** (2010). Hormone Action in the Mammary Gland. *Cold Spring Harb Perspect Biol* **2**.

**Bryant, D. M., Datta, A., Rodríguez-Fraticelli, A. E., Peränen, J., Martín-Belmonte, F. and Mostov, K. E.** (2010). A molecular network for de novo generation of the apical surface and lumen. *Nat Cell Biol* **12**, 1035-45.

**Bryant, D. M., Roignot, J., Datta, A., Overeem, A. W., Kim, M., Yu, W., Peng, X., Eastburn, D. J., Ewald, A. J., Werb, Z. et al.** (2014). A molecular switch for the orientation of epithelial cell polarization. *Dev Cell* **31**, 171-87.

**Burgoyne, R. D., Handel, S. E., Morgan, A., Rennison, M. E., Turner, M. D. and Wilde, C. J.** (1991). Calcium, the cytoskeleton and calpactin (annexin II) in exocytotic secretion from adrenal chromaffin and mammary epithelial cells. *Biochem Soc Trans* **19**, 1085-90.

**Campbell, K. and Casanova, J.** (2016). A common framework for EMT and collective cell migration. *Development* **143**, 4291-4300.

**Chen, Q. K., Lee, K., Radisky, D. C. and Nelson, C. M.** (2013). Extracellular matrix proteins regulate epithelial-mesenchymal transition in mammary epithelial cells. *Differentiation* **86**, 126-32.

**Chen, W. C. and Obrink, B.** (1991). Cell-cell contacts mediated by E-cadherin (uvomorulin) restrict invasive behavior of L-cells. *J Cell Biol* **114**, 319-27.

**Debnath, J. and Brugge, J. S.** (2005). Modelling glandular epithelial cancers in three-dimensional cultures. *Nat Rev Cancer* **5**, 675-88.

**Debnath, J., Mills, K. R., Collins, N. L., Reginato, M. J., Muthuswamy, S. K. and Brugge, J. S.** (2002). The role of apoptosis in creating and maintaining luminal space within normal and oncogene-expressing mammary acini. *Cell* **111**, 29-40.

**Ding, C., Cong, X., Zhang, Y., Li, S. L., Wu, L. L. and Yu, G. Y.** (2018).  $\beta$ -adrenoceptor activation increased VAMP-2 and syntaxin-4 in secretory granules are involved in protein secretion of submandibular gland through the PKA/F-actin pathway. *Biosci Rep* **38**.

**Druso, J. E., Endo, M., Lin, M. C., Peng, X., Antonyak, M. A., Meller, S. and Cerione, R. A.** (2016). An Essential Role for Cdc42 in the Functioning of the Adult Mammary Gland. *J Biol Chem* **291**, 8886-95.

Duan, X. L., Guo, Z., He, Y. T., Li, Y. X., Liu, Y. N., Bai, H. H., Li, H. L., Hu, X. D. and Suo, Z. W. (2020). SNAP25/syntaxin4/VAMP2/Munc18-1 Complexes in Spinal Dorsal Horn Contributed to Inflammatory Pain. *Neuroscience* **429**, 203-212.

Dumortier, J. G., Le Verge-Serandour, M., Tortorelli, A. F., Mielke, A., de Plater, L., Turlier, H. and Maître, J. L. (2019). Hydraulic fracturing and active coarsening position the lumen of the mouse blastocyst. *Science* **365**, 465-468.

Ewald, A. J., Brenot, A., Duong, M., Chan, B. S. and Werb, Z. (2008). Collective epithelial migration and cell rearrangements drive mammary branching morphogenesis. *Dev Cell* **14**, 570-81.

Ewald, A. J., Huebner, R. J., Palsdottir, H., Lee, J. K., Perez, M. J., Jorgens, D. M., Tauscher, A. N., Cheung, K. J., Werb, Z. and Auer, M. (2012). Mammary collective cell migration involves transient loss of epithelial features and individual cell migration within the epithelium. *J Cell Sci* **125**, 2638-54.

Fialka, I., Schwarz, H., Reichmann, E., Oft, M., Busslinger, M. and Beug, H. (1996). The estrogen-dependent c-JunER protein causes a reversible loss of mammary epithelial cell polarity involving a destabilization of adherens junctions. *J Cell Biol* **132**, 1115-32.

Friedl, P. and Mayor, R. (2017). Tuning Collective Cell Migration by Cell–Cell Junction Regulation. *Cold Spring Harb Perspect Biol* **9**.

Fukata, M., Kuroda, S., Nakagawa, M., Kawajiri, A., Itoh, N., Shoji, I., Matsuura, Y., Yonehara, S., Fujisawa, H., Kikuchi, A. et al. (1999). Cdc42 and Rac1 regulate the interaction of IQGAP1 with beta-catenin. *J Biol Chem* **274**, 26044-50.

Georgiou, M., Marinari, E., Burden, J. and Baum, B. (2008). Cdc42, Par6, and aPKC regulate Arp2/3-mediated endocytosis to control local adherens junction stability. *Curr Biol* **18**, 1631-8.

Gudjonsson, T., Adriance, M. C., Sternlicht, M. D., Petersen, O. W. and Bissell, M. J. (2005). Myoepithelial Cells: Their Origin and Function in Breast Morphogenesis and Neoplasia. *J Mammary Gland Biol Neoplasia* **10**, 261-72.

Hagiwara-Chatani, N., Shirai, K., Kido, T., Horigome, T., Yasue, A., Adachi, N. and Hirai, Y. (2017). Membrane translocation of t-SNARE protein syntaxin-4 abrogates ground-state pluripotency in mouse embryonic stem cells. *Sci Rep* **7**, 39868.

- Hagiwara, N., Kadono, N., Miyazaki, T., Maekubo, K. and Hirai, Y.** (2013). Extracellular syntaxin4 triggers the differentiation program in teratocarcinoma F9 cells that impacts cell adhesion properties. *Cell Tissue Res* **354**, 581-91.
- Hinck, L. and Silberstein, G. B.** (2005). Key stages in mammary gland development: The mammary end bud as a motile organ. *Breast Cancer Res* **7**, 245-51.
- Hirai, Y.** (2001). Epimorphin as a morphogen: Does a protein for intracellular vesicular targeting act as an extracellular signaling molecule? *Cell Biol Int* **25**, 193-5.
- Hirai, Y., Lochter, A., Galosy, S., Koshida, S., Niwa, S. and Bissell, M. J.** (1998). Epimorphin functions as a key morphoregulator for mammary epithelial cells. *Journal of Cell Biology* **140**, 159-169.
- Hirai, Y., Nelson, C. M., Yamazaki, K., Takebe, K., Przybylo, J., Madden, B. and Radisky, D. C.** (2007). Non-classical export of epimorphin and its adhesion to  $\alpha$ -v-integrin in regulation of epithelial morphogenesis. *J Cell Sci* **120**, 2032-43.
- Hirai, Y., Takebe, K., Takashina, M., Kobayashi, S. and Takeichi, M.** (1992). Epimorphin: a mesenchymal protein essential for epithelial morphogenesis. *Cell* **69**, 471-81.
- Hirose, Y., Shirai, K. and Hirai, Y.** (2018). Membrane-tethered syntaxin-4 locally abrogates E-cadherin function and activates Smad signals, contributing to asymmetric mammary epithelial morphogenesis. *J Cell Biochem* **119**, 7525-7539.
- Ivanova, E., Le Guillou, S., Hue-Beauvais, C. and Le Provost, F.** (2021). Epigenetics: New Insights into Mammary Gland Biology. *Genes (Basel)* **12**.
- Janda, E., Nevolo, M., Lehmann, K., Downward, J., Beug, H. and Grieco, M.** (2006). Raf plus TGF $\beta$ -dependent EMT is initiated by endocytosis and lysosomal degradation of E-cadherin. *Oncogene* **25**, 7117-30.
- Kadono, N., Hagiwara, N., Tagawa, T., Maekubo, K. and Hirai, Y.** (2015). Extracellularly Extruded Syntaxin-4 Is a Potent Cornification Regulator of Epidermal Keratinocytes. *Mol Med* **21**, 77-86.
- Kadono, N., Miyazaki, T., Okugawa, Y., Nakajima, K. and Hirai, Y.** (2012). The impact of extracellular syntaxin4 on HaCaT keratinocyte behavior. *Biochem Biophys Res Commun* **417**, 1200-5.

- Kiener, H. P., Niederreiter, B., Lee, D. M., Jimenez-Boj, E., Smolen, J. S. and Brenner, M. B.** (2009). Cadherin 11 promotes invasive behavior of fibroblast-like synoviocytes. *Arthritis Rheum* **60**, 1305-10.
- Kota, P., Terrell, E. M., Ritt, D. A., Insinna, C., Westlake, C. J. and Morrison, D. K.** (2019). M-Ras/Shoc2 signaling modulates E-cadherin turnover and cell-cell adhesion during collective cell migration. *Proc Natl Acad Sci U S A* **116**, 3536-3545.
- Kowalczyk, A. P. and Nanes, B. A.** (2012). Adherens junction turnover: regulating adhesion through cadherin endocytosis, degradation, and recycling. *Subcell Biochem* **60**, 197-222.
- Kuroda, S., Fukata, M., Nakagawa, M., Fujii, K., Nakamura, T., Ookubo, T., Izawa, I., Nagase, T., Nomura, N., Tani, H. et al.** (1998). Role of IQGAP1, a target of the small GTPases Cdc42 and Rac1, in regulation of E-cadherin-mediated cell-cell adhesion. *Science* **281**, 832-5.
- Lamouille, S., Xu, J. and Derynck, R.** (2014). Molecular mechanisms of epithelial-mesenchymal transition. *Nat Rev Mol Cell Biol* **15**, 178-96.
- Lehnert, L., Lerch, M. M., Hirai, Y., Kruse, M. L., Schmiegel, W. and Kalthoff, H.** (2001). Autocrine stimulation of human pancreatic duct-like development by soluble isoforms of epimorphin in vitro. *J Cell Biol* **152**, 911-22.
- Leibfried, A., Fricke, R., Morgan, M. J., Bogdan, S. and Bellaiche, Y.** (2008). Drosophila Cip4 and WASp define a branch of the Cdc42-Par6-aPKC pathway regulating E-cadherin endocytosis. *Curr Biol* **18**, 1639-48.
- Macias, H. and Hinck, L.** (2012). Mammary Gland Development. *Wiley Interdiscip Rev Dev Biol* **1**, 533-57.
- Martín-Belmonte, F., Yu, W., Rodríguez-Fraticelli, A. E., Ewald, A. J., Werb, Z., Alonso, M. A. and Mostov, K.** (2008). Cell-polarity dynamics controls the mechanism of lumen formation in epithelial morphogenesis. *Curr Biol* **18**, 507-13.
- Meng, W., Mushika, Y., Ichii, T. and Takeichi, M.** (2008). Anchorage of microtubule minus ends to adherens junctions regulates epithelial cell-cell contacts. *Cell* **135**, 948-59.
- Mills, E. S. and Topper, Y. J.** (1970). Some ultrastructural effects of insulin, hydrocortisone, and prolactin on mammary gland explants. *J Cell Biol* **44**, 310-28.

**Murata, K., Baasanjav, A., Kwon, C., Hashimoto, M., Ishida, J. and Fukamizu, A.** (2015). Angiotensin II accelerates mammary gland development independently of high blood pressure in pregnancy-associated hypertensive mice. *Physiol Rep* **3**.

**Nagafuchi, A., Ishihara, S. and Tsukita, S.** (1994). The roles of catenins in the cadherin-mediated cell adhesion: functional analysis of E-cadherin-alpha catenin fusion molecules. *J Cell Biol* **127**, 235-45.

**Nagafuchi, A., Shirayoshi, Y., Okazaki, K., Yasuda, K. and Takeichi, M.** (1987). Transformation of cell adhesion properties by exogenously introduced E-cadherin cDNA. *Nature* **329**, 341-3.

**Neumann, N. M., Perrone, M. C., Veldhuis, J. H., Huebner, R. J., Zhan, H., Devreotes, P. N., Brodland, G. W. and Ewald, A. J.** (2018). Coordination of Receptor Tyrosine Kinase Signaling and Interfacial Tension Dynamics Drives Radial Intercalation and Tube Elongation. *Dev Cell* **45**, 67-82 e6.

**Okugawa, Y. and Hirai, Y.** (2008). Overexpression of extracellular epimorphin leads to impaired epidermal differentiation in HaCaT keratinocytes. *J Invest Dermatol* **128**, 1884-93.

**Paine, I. S. and Lewis, M. T.** (2017). The Terminal End Bud: the Little Engine that Could. *J Mammary Gland Biol Neoplasia* **22**, 93-108.

**Radisky, D. C., Stallings-Mann, M., Hirai, Y. and Bissell, M. J.** (2009). Single proteins might have dual but related functions in intracellular and extracellular microenvironments. *Nat Rev Mol Cell Biol* **10**, 228-34.

**Roignot, J., Peng, X. and Mostov, K.** (2013). Polarity in Mammalian Epithelial Morphogenesis. *Cold Spring Harb Perspect Biol* **5**.

**Sako-Kubota, K., Tanaka, N., Nagae, S., Meng, W. and Takeichi, M.** (2014). Minus end-directed motor KIFC3 suppresses E-cadherin degradation by recruiting USP47 to adherens junctions. *Mol Biol Cell* **25**, 3851-60.

**Shamir, E. R. and Ewald, A. J.** (2015). Adhesion in Mammary Development: Novel Roles for E-Cadherin in Individual and Collective Cell Migration. *Curr Top Dev Biol* **112**, 353-82.

**Shirai, K., Hagiwara, N., Horigome, T., Hirose, Y., Kadono, N. and Hirai, Y.** (2017). Extracellularly Extruded Syntaxin-4 Binds to Laminin and Syndecan-1 to Regulate Mammary Epithelial Morphogenesis. *J Cell Biochem* **118**, 686-698.

**Smoczyński, M.** (2017). Role of Phospholipid Flux during Milk Secretion in the Mammary Gland. *J Mammary Gland Biol Neoplasia* **22**, 117-129.

**Song, S., Eckerle, S., Onichtchouk, D., Marrs, J. A., Nitschke, R. and Driever, W.** (2013). Pou5f1-dependent EGF expression controls E-cadherin endocytosis, cell adhesion, and zebrafish epiboly movements. *Dev Cell* **24**, 486-501.

**Sternlicht, M. D., Kouros-Mehr, H., Lu, P. and Werb, Z.** (2006). Hormonal and local control of mammary branching morphogenesis. *Differentiation* **74**, 365-81.

**Takeichi, M.** (2014). Dynamic contacts: rearranging adherens junctions to drive epithelial remodelling. *Nat Rev Mol Cell Biol* **15**, 397-410.

**Vidi, P. A., Bissell, M. J. and Lelièvre, S. A.** (2013). Three-Dimensional Culture of Human Breast Epithelial Cells: The How and the Why. *Methods Mol Biol* **945**, 193-219.

**Woltjen, K., Michael, I. P., Mohseni, P., Desai, R., Mileikovsky, M., Hämäläinen, R., Cowling, R., Wang, W., Liu, P., Gertsenstein, M. et al.** (2009). piggyBac transposition reprograms fibroblasts to induced pluripotent stem cells. *Nature* **458**, 766-70.

**Zhang, M., Chen, D., Zhen, Z., Ao, J., Yuan, X. and Gao, X.** (2018). Annexin A2 positively regulates milk synthesis and proliferation of bovine mammary epithelial cells through the mTOR signaling pathway. *J Cell Physiol* **233**, 2464-2475.



## Figures

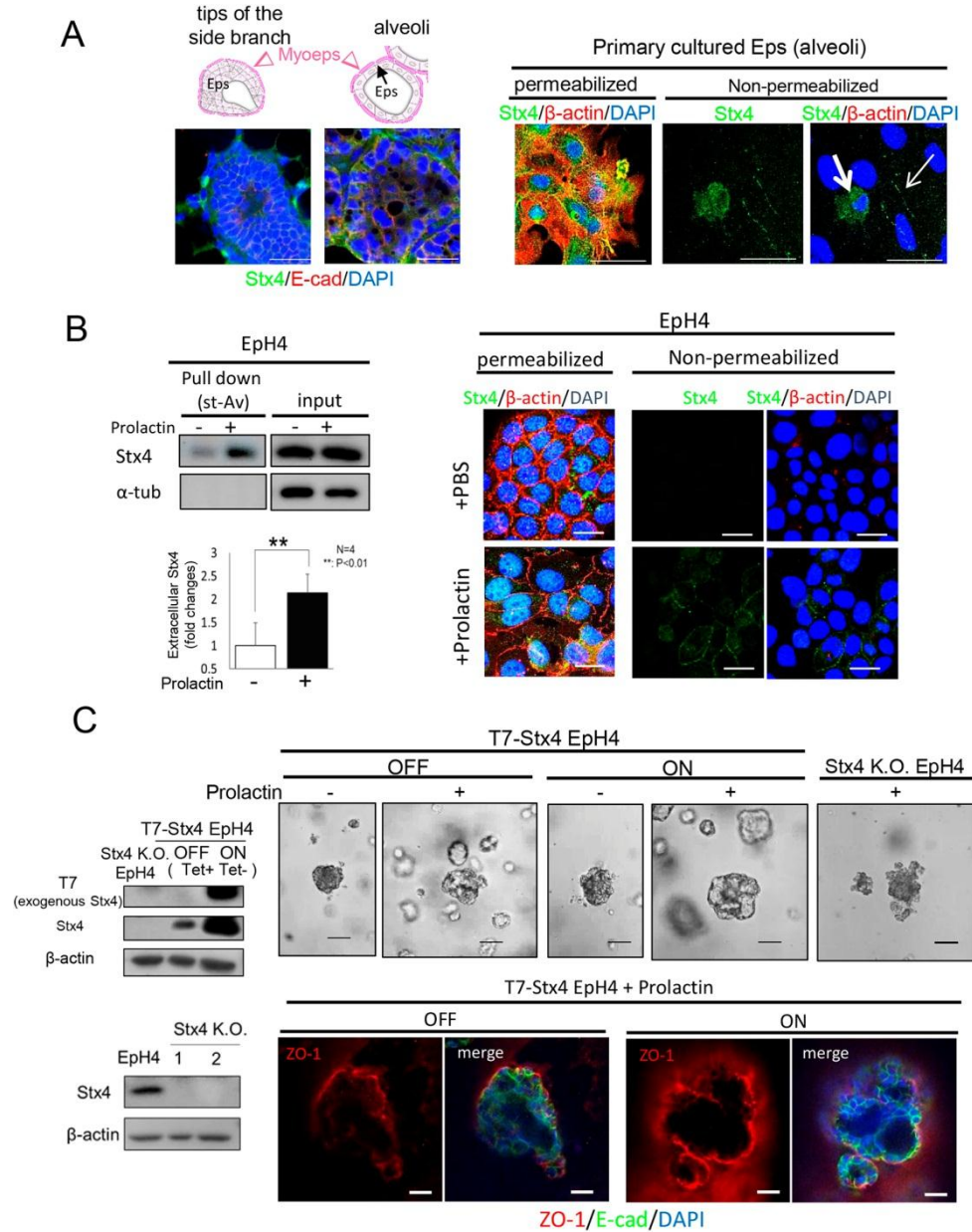


**Fig. 1. Effect of syntaxin4 on three-dimensional morphogenesis of mammary gland epithelia.** A, Left upper, schematic diagrams of a tip of side branch (multilayered epithelia) and cystic alveoli in the lobule (single layered epithelial cells). The luminal epithelial cells (Eps, arrow) are surrounded by a layer of myoepithelial cells (Myoeps, arrow head). Left lower, tip of a side branch or possibly a terminal end bud (7 weeks of age), and alveoli (lactation period day 1) in the mouse mammary gland were stained for syntaxin4 (Stx4, green) and E-cadherin (E-cad, red). Nuclei were counterstained

with DAPI. Bars, 25  $\mu\text{m}$ . Right, Mammary Eps were isolated from developing alveoli, cultured with prolactin (1  $\mu\text{g}/\text{mL}$ ), and stained for total (permeabilized) or cell surface (non-permeabilized)  $\beta$ -actin (red) and syntaxin4 (green). Bars, 50  $\mu\text{m}$ . B, EpH4 cells stimulated with prolactin extruded syntaxin4 at the cell surface. Left, biotinylated surface proteins retrieved with NeutrAvidin-beads (pull down) from lysate of EpH4 cells (input) were tested for syntaxin4 and cytoplasmic  $\alpha$ -tubulin.  $N = 4$ , \*\*;  $p < 0.01$ . Right, EpH4 cells cultured with (+) or without (+ PBS) prolactin were stained for total (permeabilized) or cell surface (non-permeabilized)  $\beta$ -actin (red) and syntaxin-4 (green). Nuclei were counterstained with DAPI. Bars, 25  $\mu\text{m}$ . Stimulation with prolactin for 24 h led to the translocation of syntaxin4 across the cell membrane in part of EpH4 cells. C, Left upper, EpH4 cells with inducible expression of T7 tagged syntaxin4 (T7-Stx4 EpH4) and those with complete depletion of syntaxin4 (Stx4 K.O. EpH4) Upon removal of tetracycline (tet -) (ON), T7-Stx4 EpH4 cells expressed exogenous syntaxin4. Left lower, Stx4 K.O. EpH4 cells generated by different gRNAs (clone1 and 2). Right upper, morphology of aggregates of EpH4 derivatives (T7-Stx4 EpH4 with Stx4-OFF, T7-Stx4 EpH4 with Stx4-ON, Stx4 K.O. EpH4 cells) cultured in Matrigel with (+) or without (-) prolactin for five days. Bars, 50  $\mu\text{m}$ . In response to prolactin, aggregates of the T7-Stx4 EpH4 cells produced multiple lumens, the expansion speed of which roughly depended on the expression amount of syntaxin4. By contrast, Stx4 K.O. EpH4 cells never underwent such a cellular arrangement. As the phenotypic appearance was indistinguishable between clone 1 and 2, only that of clone 2 is shown. Right lower, aggregates of T7-Stx4 EpH4 cells cultured in the presence of prolactin in Matrigel were stained for E-cadherin (green) and ZO-1 (red). Treatment with prolactin induced formation of multiple lumen, regardless of the induction of exogenous syntaxin4, however, clear apicobasal polarity was not established as judged by the localization of ZO-1. Bars, 20  $\mu\text{m}$ .

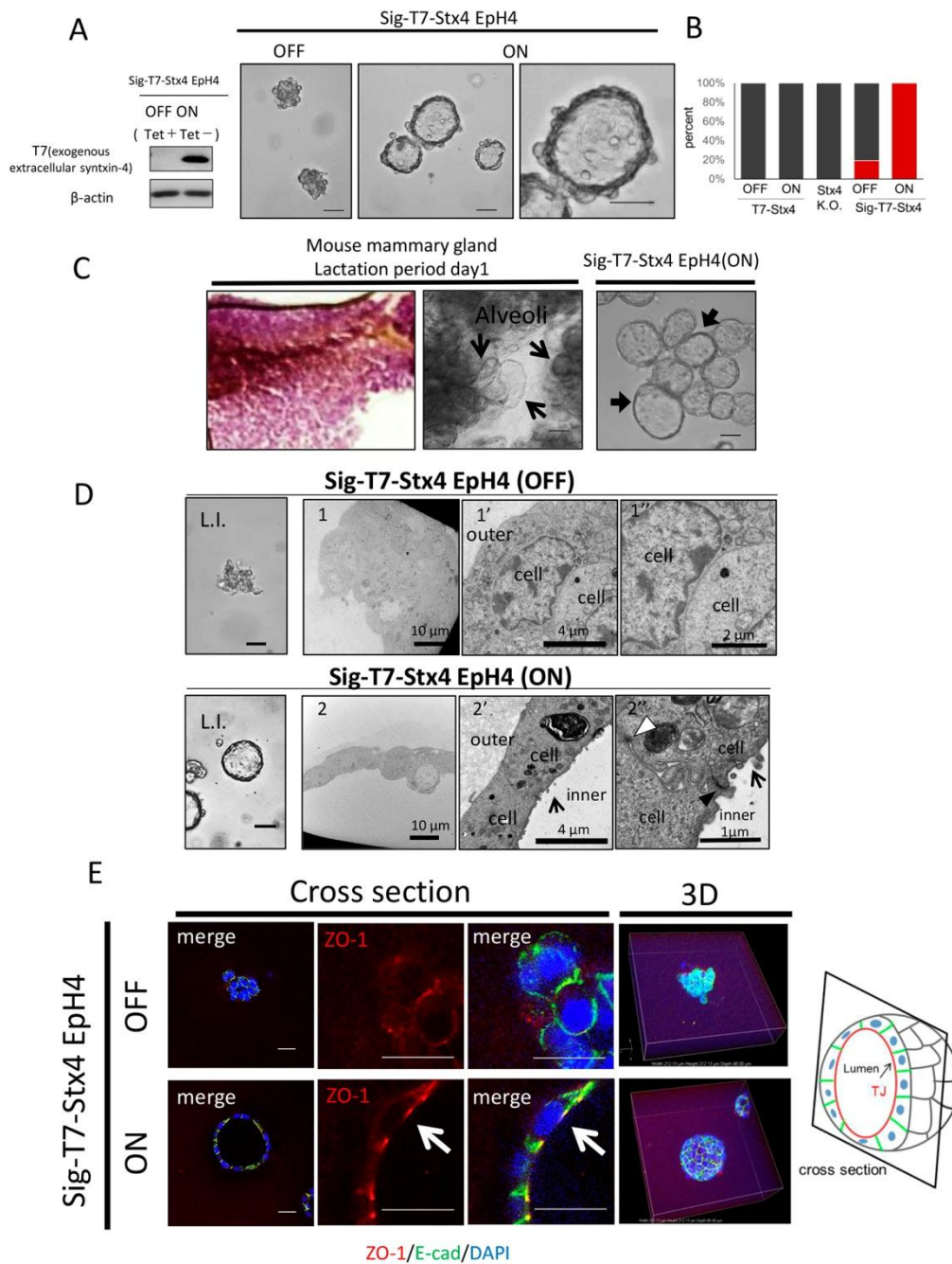


**Fig. 2. Analyses of the cystic structures induced by extracellular syntaxin4.**

A, Aggregates of EpH4 cells, which had been introduced with a construct for tet-repressible T7-Syntaxin4 containing N-terminal fusion of a signal peptide (Sig-T7-Stx4-EpH4) (left), were embedded in Matrigel and analyzed for morphological characteristics on day 5. In response to forced expression of extracellular syntaxin4, dramatic cellular arrangements of the cystic structures were induced even in a prolactin-free medium. Bars, 50  $\mu$ m. B, Ratio of cell aggregates with large (more

than 30  $\mu\text{m}$  in diameter) central lumen (red). C, Left, murine mammary gland at lactation period day 1 stained with Carmine Alum solution. Middle, microscopic images of the alveoli (thin arrows) in the enzymatically dissociated glands are also shown. Right, Overall structure of the syntaxin4-induced cystic architecture (thick arrows) resembles that of alveoli of a lactating gland. Bars, 50  $\mu\text{m}$ . D, Microstructural features of EpH4 cell aggregates with (Stx4 ON, 2, 2', and 2'') or without (Stx4 OFF, 1, 1', and 1'') extracellular expression of Stx4 (Sig-T7-Stx4). Scale bar is indicated in each image. L.I.: microscopic images for each category. Bars, 50  $\mu\text{m}$ . While the cells without extracellular syntaxin4 remained as tightly packed cell clumps, those with extracellular syntaxin4 formed single cell layered-cysts possessing developed desmosomes (white arrowhead), polarized tight junctions (TJs, black arrowhead) and microvilli facing toward luminal spaces (arrows). E, Left, EpH4 cysts induced by Sig-T7-Stx4 were stained for TJ protein ZO-1 (red) and E-cadherin (green). 3D, reconstructed three dimensional images. Nuclei were counterstained with DAPI (blue). ZO-1 was localized at lumen-proximal regions of the cell membrane (arrows) in cells with extracellular syntaxin4 (ON). Bars, 20  $\mu\text{m}$ . Right, Schematic diagram of the cystic architecture induced by extracellular syntaxin4.

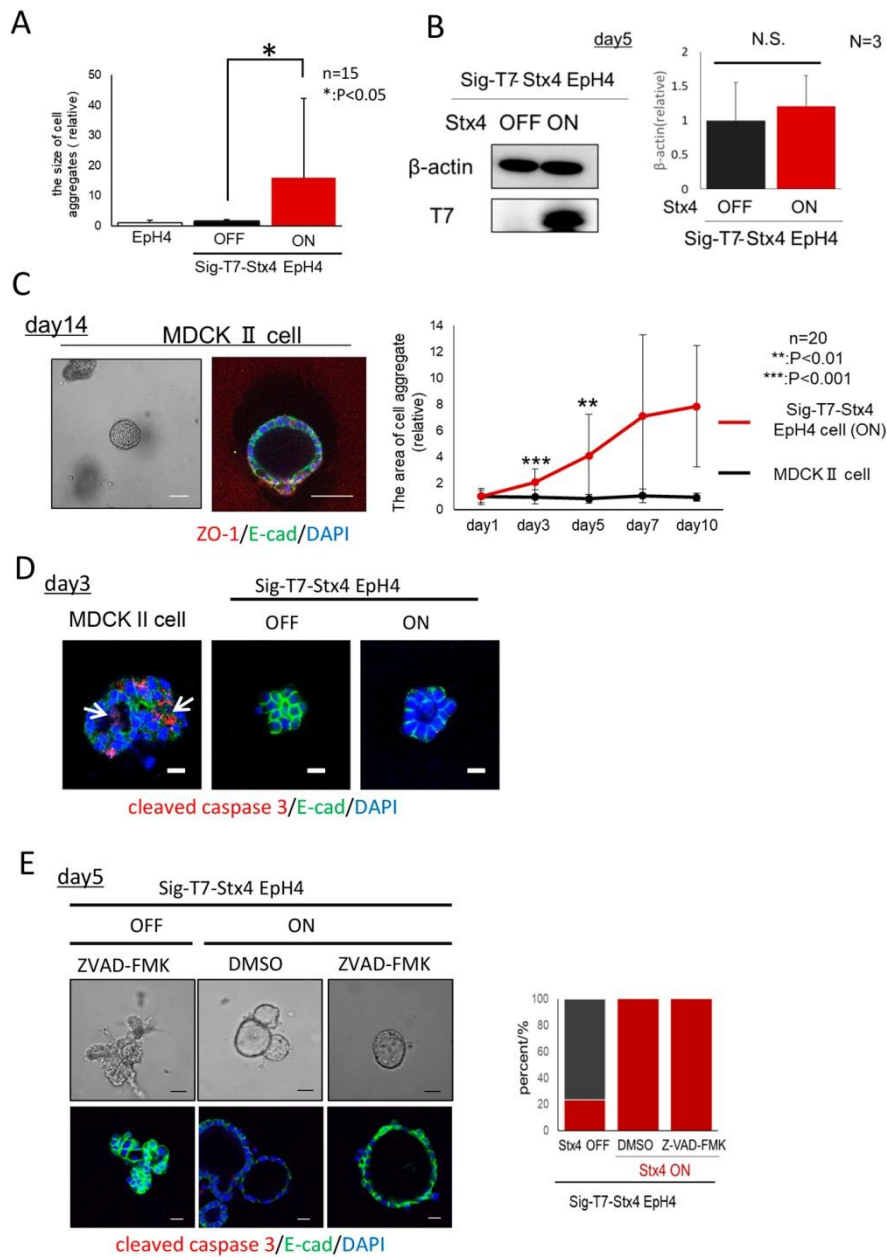


**Fig. 3. Comparison of cysts induced in EpH4 cells by syntaxin4 and in MDCK II cells without syntaxin4.**

A, Relative size of EpH4 cell aggregates with (ON) and without (OFF) extracellular syntaxin4 after 5 days of incubation.  $n = 15$ ,  $*$ ;  $p < 0.05$ . B, The amount of  $\beta$ -actin, a representative of total cell number, was analyzed to determine cellular proliferation in aggregates with (ON) and without (OFF) extracellular syntaxin4.  $N = 3$ . Extracellular syntaxin4 led to cyst expansion without cell proliferation. C, Cyst formation in cell aggregates of another epithelial cell line, MDCKII, in Matrigel. Left, microscopic and immunofluorescence images. Green, E-cadherin. Red, ZO-1. Bars,

50  $\mu\text{m}$ . Right, time-dependent size changes in aggregates of Sig-T7-Stx4 EpH4 (Stx4 ON) (red) and MDCK II (gray).  $n = 20$ , \*\*,  $p < 0.01$ , \*\*\*,  $p < 0.001$ . While the cyst size of the aggregates of Sig-T7-Stx4 EpH4 dramatically increased in a week, that of MDCK II remained practically unchanged. D, Aggregates of MDCK II and Sig-T7-Stx4 EpH4 cells were cultured for 3 days and stained for cleaved-caspase-3 (red) and E-cadherin (green). Cleaved-caspase-3 was detected in the growing lumen of MDCK II cell aggregates (arrows), but not of Sig-T7-Stx4 EpH4. Bars, 50  $\mu\text{m}$ . E, Left, Treatment with ZVAD-FMK, a pan-caspase inhibitor (20  $\mu\text{M}$ ), for five days did not prevent cyst formation (Stx4 ON) in Sig-T7-Stx4 EpH4 aggregates. DMSO, vehicle control. Upper panel, Microscopic images. Lower panel, transverse sections stained for E-cadherin (green) and cleaved-caspase3 (red). Nuclei were counterstained with DAPI. Bars, 50  $\mu\text{m}$  (upper panel) and 20  $\mu\text{m}$  (lower panel). Right, quantification of the ZVAD-FMK effect on lumen formation by extracellular syntaxin4. Sig-T7-Stx4 EpH4 cells developed palpable lumens (red), even in the presence of a pan-caspase inhibitor.



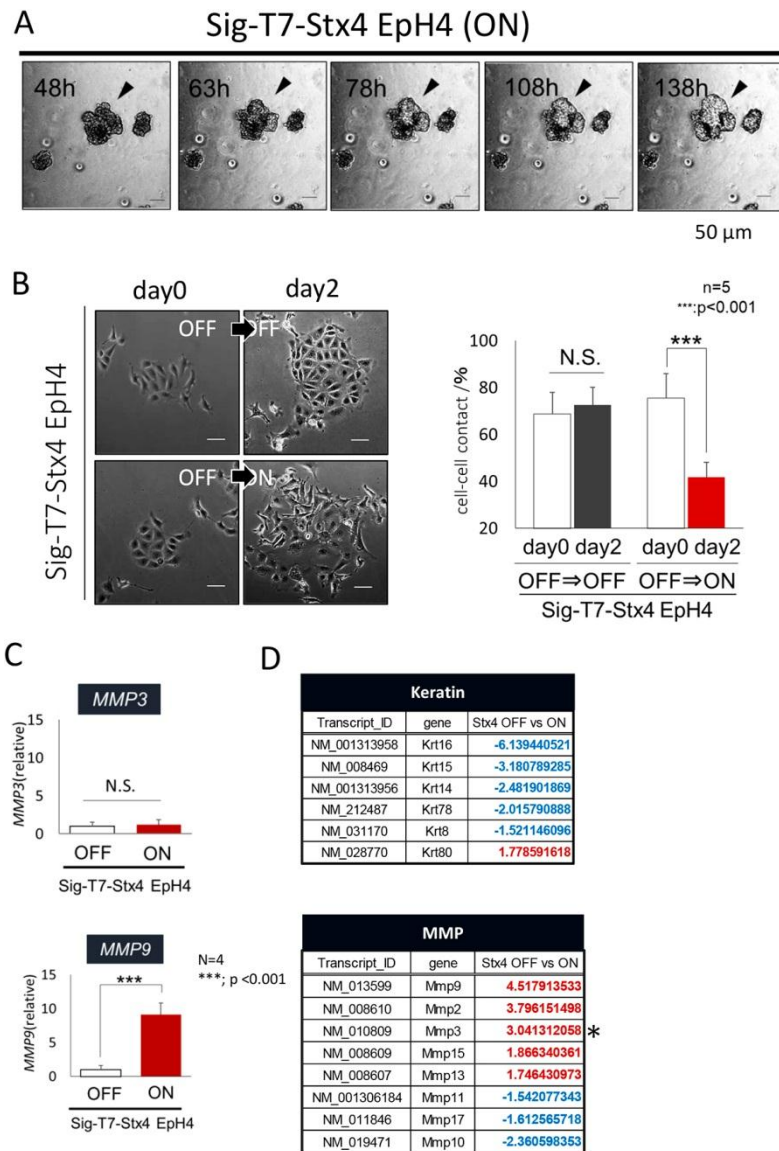
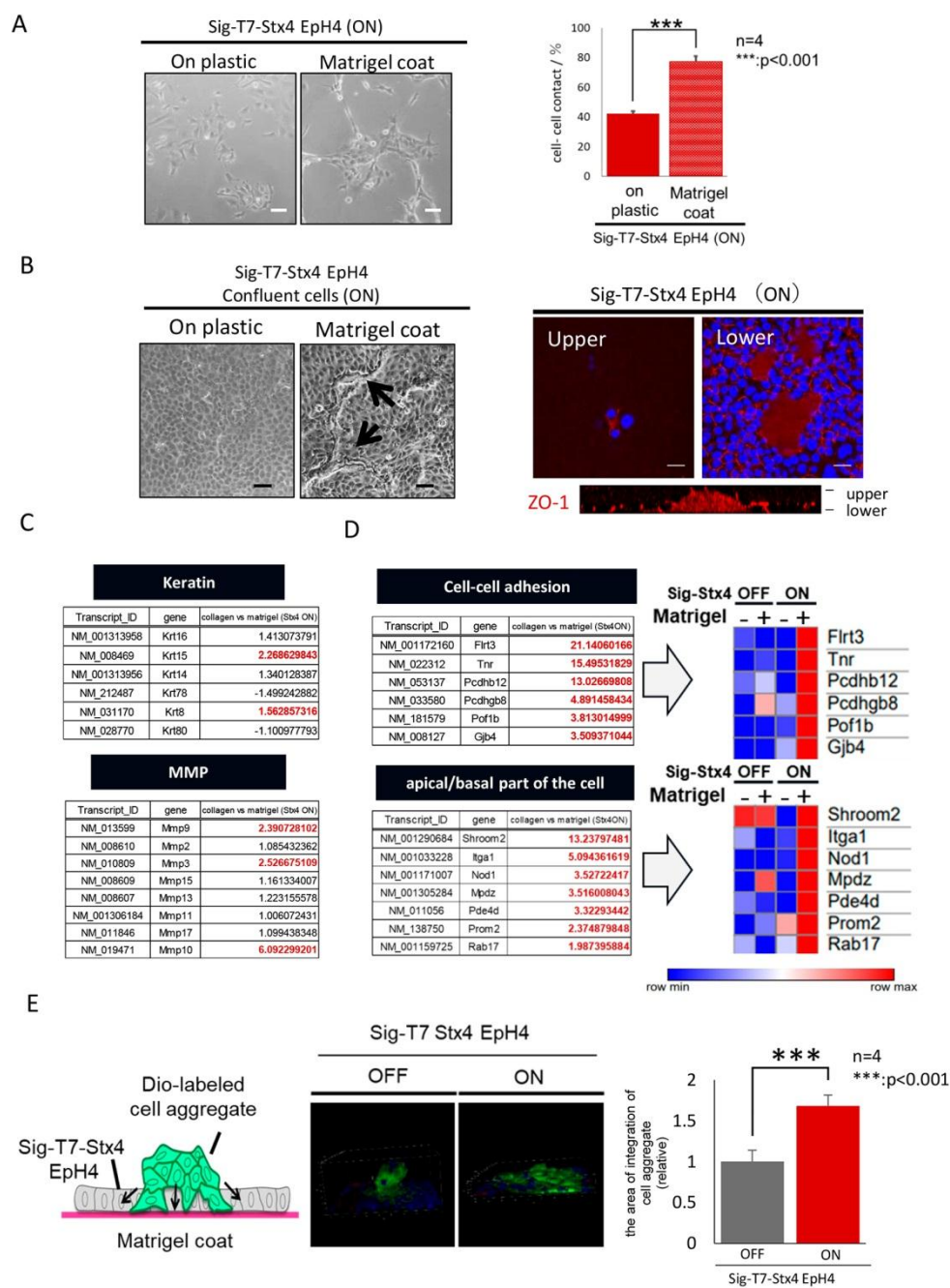


**Fig. 4. Behaviors of individual EpH4 cells in response to extracellular syntaxin4.**

A, Time-lapse images of aggregates of Sig-T7-Stx4 EpH4 (ON) in Matrigel. After 48 h of induction, the onset of cellular arrangement towards the formation of the cystic structure became apparent. Subsequently, the overall size of the cell aggregates gradually increased as the inner portion became transparent. Bars, 50  $\mu$ m. B, Left, microscopic images of Sig-T7-Stx4 EpH4 cultured on dishes with (ON) or without (OFF) induction of extracellular syntaxin4 for two days. Bars, 50  $\mu$ m. Right, ratio of the cells exhibiting the direct cell-cell contact. The number of cells adhering to each other was counted on days 0 and 2.  $n = 5$ , \*\*\*;  $p < 0.001$ . Extracellular syntaxin4 disrupted intercellular adhesion and elicited migratory responses. C, mRNA expression of *Mmp-9* and *Mmp3* in EpH4 cells with (ON) or without (OFF) extracellular syntaxin4.  $N=4$ ; \*\*\*;  $p < 0.001$ . D, RNA-sequence

analyses revealed the induction of the onset of EMT-like cell behaviors by extracellular syntaxin4. Among the comprehensive data sets, all genes showing more than 1.5-fold changes in the word category “keratin (11 keratins in total)” or “MMP (13 MMPs in total)” were extracted and listed. The upregulated and downregulated genes in response to extracellular syntaxin4 are shown in red and blue, respectively. \*, While *Mmp3* is listed as one of the upregulated genes, qRT-PCR analysis did not detect this change (see C).

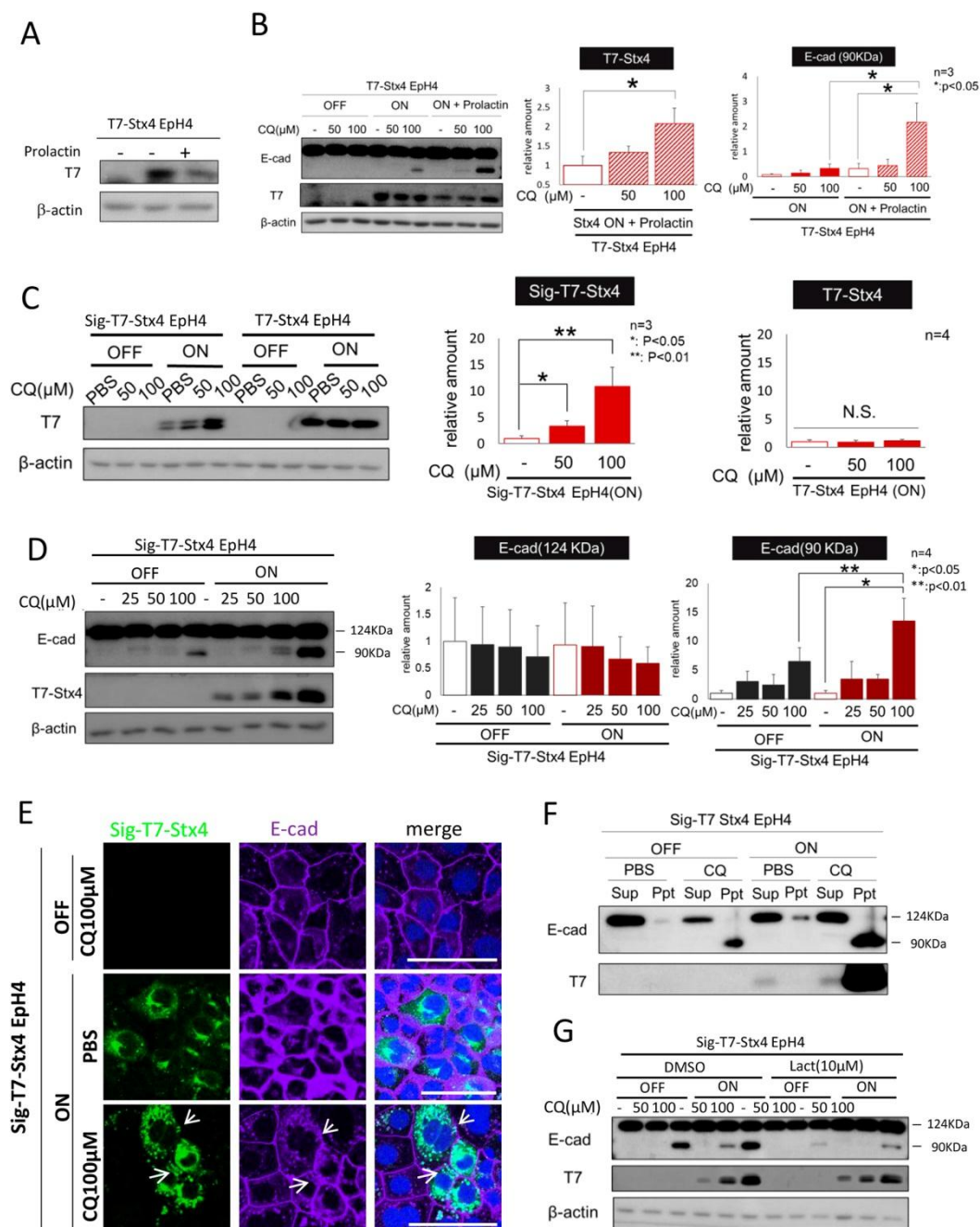




**Fig. 5. Distinct behaviors in syntaxin4-expressing EpH4 cells faced on Matrigel**

A, Left, microscopic images of growing Sig-T7-Stx4 EpH4 cells (ON) on dishes coated with and without Matrigel. Bars, 20  $\mu$ m. Right, ratio of cells exhibiting direct cell-cell contact on day 2. The reduction of intercellular adhesion induced by extracellular syntaxin4 was apparently recovered if cells directly adhered to Matrigel. B, Confluent Sig-T7-Stx4 EpH4 cells (ON) on dishes coated with and without Matrigel. Left, microscopic images. Right, Cells in the upper and lower planes were

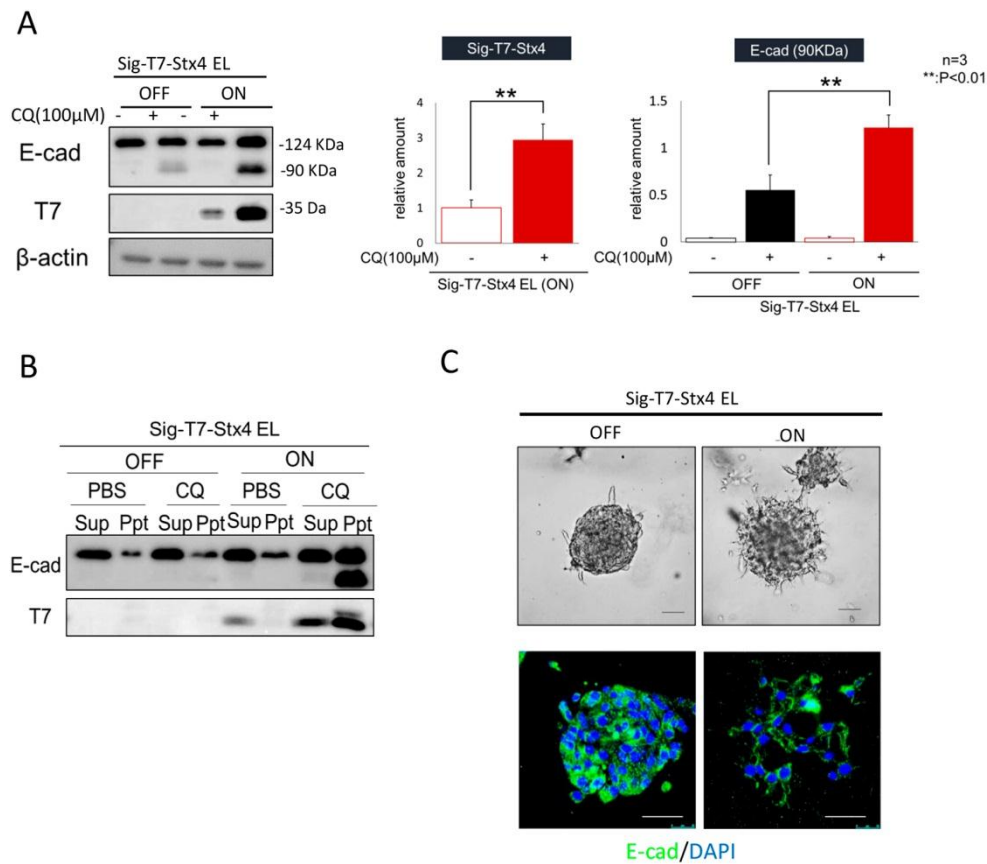
stained for ZO-1 and DAPI. The z-stack image for ZO-1 is presented below. Bars, 50  $\mu$ m. The cells on Matrigel with extracellular syntaxin4 retained the intercellular adhesion and often formed enclosed dome-like structures (arrows). C, RNA-sequencing analyses of Sig-T7-Stx4 EpH4 (ON) cultured on Matrigel versus collagen control. With regard to all keratin and MMP genes showing more than 1.5-fold changes in response to extracellular syntaxin4 (Fig. 4D), expression of only *Krt15* and *Krt8* was restored, but those of *Mmp9*, *Mmp3*, and *Mmp10* were further facilitated by Matrigel. Genes showing significant upregulation (more than 1.5-fold) are colored red. D, Left, genes showing significant changes in the word category “cell-cell adhesion (top six genes in descending order, from 65 genes in total)” and “apical/basal part of the cell (seven genes in descending order, from 31 genes in total)” appeared to be upregulated when cells with extracellular syntaxin4 (ON) were affected simultaneously by Matrigel. Right, Heat map analysis of these genes demonstrates synergistic effects of extracellular syntaxin4 and Matrigel on the acquisition of unique epithelial characteristics. E, Left, reconstructed 3D images of the integration of cell aggregates into a single cell layer on Matrigel. The floating aggregates of Sig-T7-Stx4 EpH4 pre-labeled with DiO (green) were seeded onto a confluent cell sheet on Matrigel, followed by five days of incubation with (ON) or without (OFF) induction of extracellular syntaxin4. Red, E-cadherin. Bars, 50  $\mu$ m. Right, relative area of Dio-labeled cells integrated into Matrigel-bound cell sheets.  $n = 4$ , \*\*\*;  $p < 0.001$ . The cell aggregates free from Matrigel smoothly integrated into the Matrigel-adherent confluent cell sheet if they expressed extracellular syntaxin4.



**Fig. 6. Effect of extracellularly extruded syntaxin4 on E-cadherin expression.**

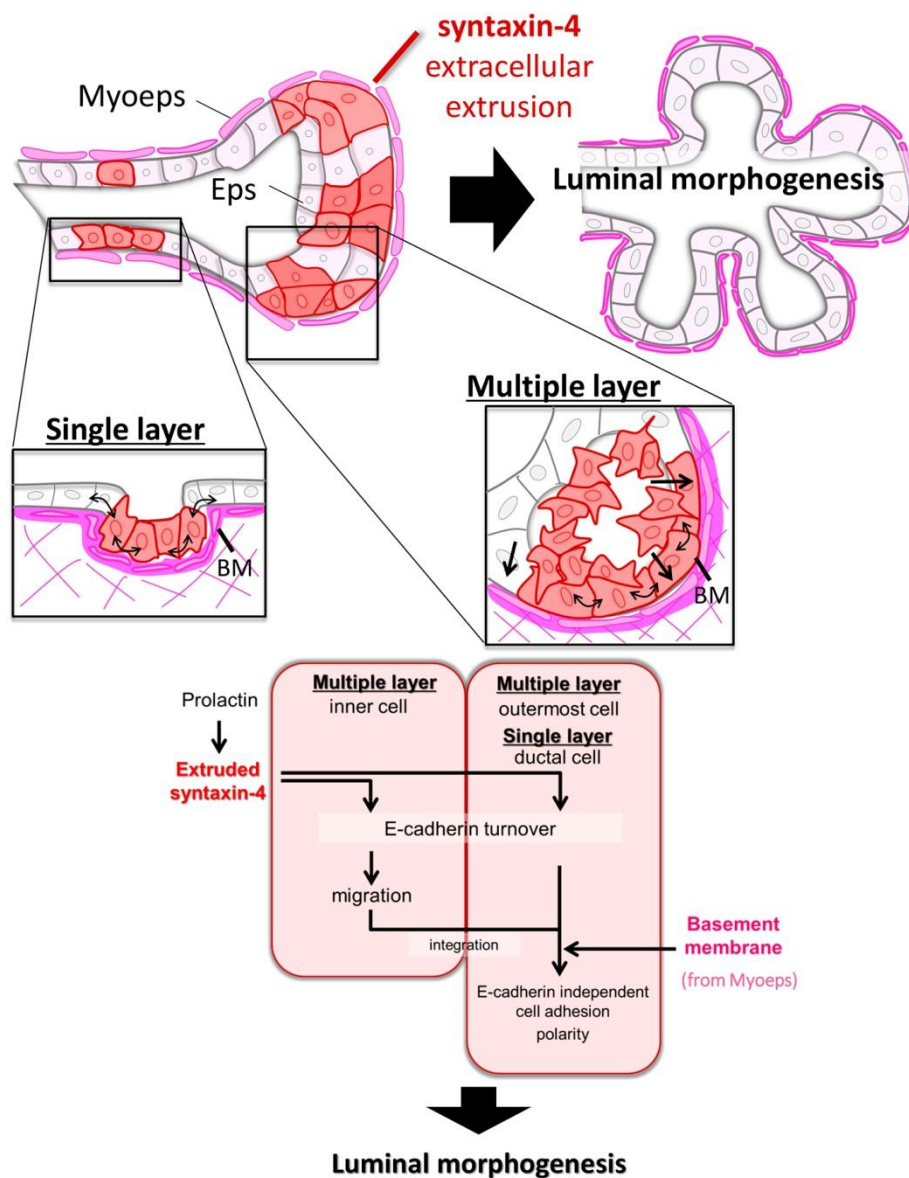
A, The amount of syntaxin4 (without the signal peptide) in the T7-Stx4 EpH4 cells was decreased by prolactin, which provoked extracellular translocation of syntaxin4.  $\beta$ -actin was used as an internal control. B, Left, The decrease in syntaxin4 (A) was ascribed to lysosomal degradation, as judged by the treatment with chloroquine (CQ), a potent inhibitor of lysosomal degradation. Treatment with prolactin coincidentally increased the 90 kDa form of E-cadherin, which is readily degraded in

lysosomes. Right, quantification of the effects of CQ. n = 3, \*, p < 0.05. C, Left, Extracellularly expressed syntaxin4 (Sig-T7-Stx4), but not the intact form of syntaxin4 (T7-Stx4), was actively degraded in lysosomes, even in the absence of prolactin. Right, CQ-dependent changes in the amount of extracellular (Sig-T7-Stx4, n = 3) and intact (T7-Stx4, n = 4) forms of exogenous syntaxin4 (ON). \*, p < 0.05, \*\*, p < 0.01. D, E-cadherin expression in Sig-T7-Stx4 cells treated with CQ for 12 h. Left, the amount of cleaved E-cadherin (90 kDa), which is readily degraded in lysosomes, was significantly higher in cells with extracellular syntaxin4. Right, CQ-dependent changes in the amount of intact (124 kDa) and cleaved (90 kDa) forms of E-cadherin. n = 4, \*, p < 0.05, \*\*, p < 0.01. E, CQ-treated Sig-T7-Stx4 EpH4 cells (ON) were stained for E-cadherin (magenta) and syntaxin4 (T7, green). In the presence of CQ, E-cadherin and syntaxin4 were co-localized in the cytoplasm (arrows). Bars, 20  $\mu$ m. F, Sig-T7-Stx4 EpH4 cells that were cultured with or without CQ (CQ or PBS alone, respectively) were treated with a lysis buffer, and the soluble (Sup) and insoluble (Ppt) fractions were tested for E-cadherin and extracellular syntaxin4. Both cleaved E-cadherin (90 kDa) and extracellular syntaxin4 were detectable almost exclusively in the insoluble fraction. G, Treatment of cells with a proteasome inhibitor, lactacystin (10  $\mu$ M), dramatically reduced the appearance of 90 kDa E-cadherin.



**Fig. 7. Validation of functional coordination model by syntaxin4 and laminin**

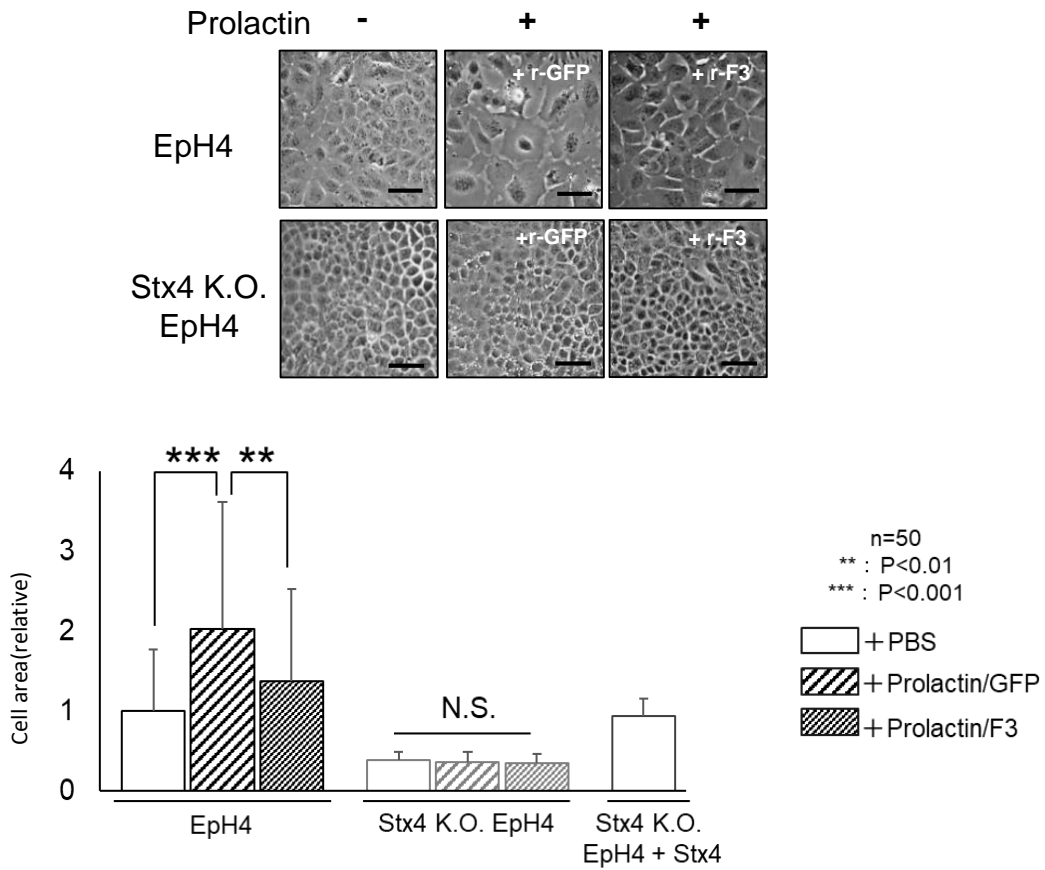
A, Left, L cells expressing exogenous E-cadherin (EL cells), which display intercellular adhesive properties only with E-cadherin, were stably transfected with the tet-regulatable Sig-T7-Stx4 construct (Sig-T7-Stx4-EL). EL cells readily produced the degraded form of E-cadherin (90 kDa) when they expressed extracellular syntaxin4. Right, quantification of exogenous extracellular syntaxin4 and 90 kDa E-cadherin. N = 3, \*\*, p < 0.01. B, Expression of extracellular syntaxin4 conferred the characteristic feature of insolubility upon E-cadherin expression. In response to exogenous extracellular syntaxin4 (ON), EL cells produced 90 kDa E-cadherin, which was detectable in the insoluble (Ppt), but not in the soluble (Sup) fraction with extracellular syntaxin4. C, Aggregates of Sig-T7-Stx4-EL cells were cultured for 7 days in Matrigel. Upper, light microscopy images. Lower, immunostained for E-cadherin (green) and nuclei (blue). EL cells, which adhere each other solely by E-cadherin and are much less responsive to basement membrane (BM) signals than Eph4 cells, were gradually disseminated and scattered in Matrigel in response to the extracellular expression of syntaxin4. Bars, 25  $\mu$ m.



**Fig. 8. Schematic diagram of functional coordination model by syntaxin4 and basement membrane components in the mammary epithelial morphogenesis.**

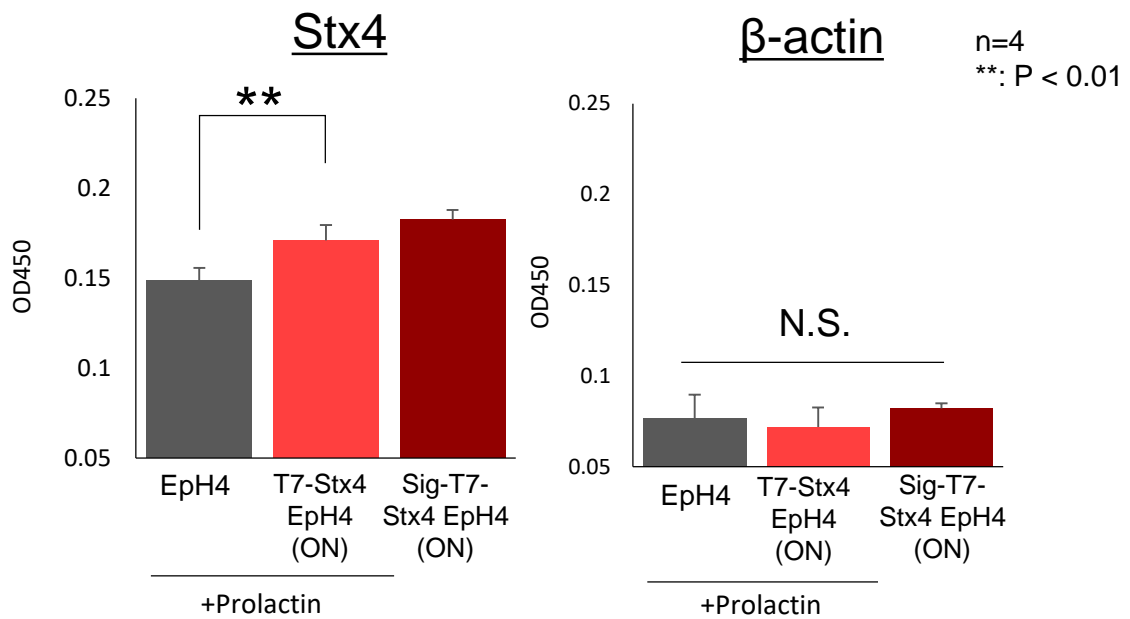
In response to the lactogenic hormone prolactin, cells in certain areas of the mammary epithelia (Eps) extrude syntaxin4, which actively triggers E-cadherin turnover and induces dramatic cellular arrangements. Cell populations that are situated away from BM-producing myoepithelial cells (Myoeps), such as at the tip of side branches, actively migrate outward and integrate into the outermost cell layers facing to the BM-producing Myoeps. Concurrently, cells faced with BM-producing Myoeps, such as in the single layered ducts or the outermost cell population in multiple layered Eps, reinforce E-cadherin-independent intercellular adhesion and establish apicobasal polarity to undergo a dramatic cellular arrangement for the formation of well-polarized cystic structures.





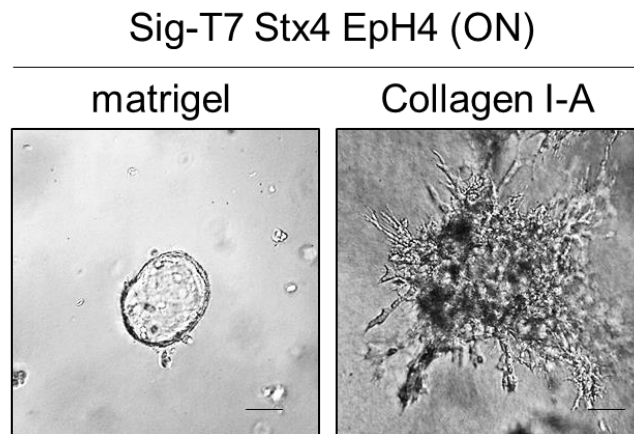
**Fig. S1.** Prolactin induced flattened morphology in parent EpH4 cells, but not in Stx4 K.O. EpH4 cells, which was blocked by the addition of membrane-impermeable syntaxin4 antagonist r-F3 (Hirose et al., 2017), but not of r-GFP control (50  $\mu$ g/ml). As Stx4 K.O. clones generated by different gRNAs behaved similarly and exogenous syntaxin4 could be expressed in clone2, the cell size was quantitated only for clone2. Compared to parent EpH4 cells, the size of Stx4 K.O. cells was apparently small, however, re-expression of syntaxin4 recovered the cell size. Bars, 50  $\mu$ m. Area occupied by a cell is shown. n= 40, \*\*\*, p< 0.001, \*\*, p< 0.01.

|  | EpH4<br>+prolactin | T7-Stx4 EpH4<br>(ON)<br>+prolactin | Sig-T7-Stx4<br>EpH4(ON) |
|--|--------------------|------------------------------------|-------------------------|
| Cells with extracellular<br>syntaxin-4 | partial            | partial                            | total                   |
| phenotype                              | multiple<br>lumen  | multiple<br>lumen                  | single<br>lumen         |

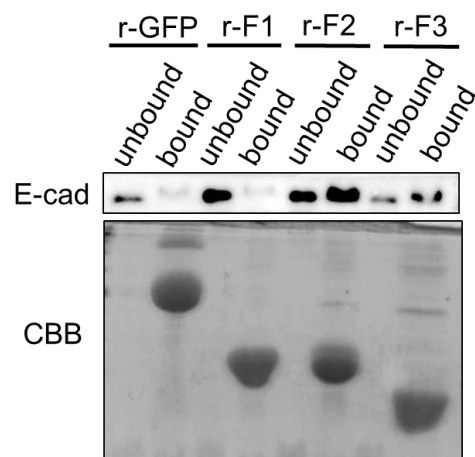


**Fig. S2.** Upper, the relationship between the mode of expression of extracellular syntaxin-4 and the phenotype. Lower, amount of extracellular syntaxin4 (Stx4) in parental EpH4 cells with prolactin, T7-Stx4 EpH4 cells (ON) with prolactin, and Sig-T7 Stx4 EpH4 cells (ON) without prolactin. Non-permeabilized cells in 96-well plate were incubated with primary antibody against syntaxin4 or β-actin, and with HRP-conjugated secondary antibodies. After excessive washing with TBS, amount of syntaxin4 or β-actin on the cell surface was quantified with TMB solution (Scy Tek, UT, USA) using the plate reader (Thermo Scientific, Finland) . n = 4. \*\*: P < 0.01. As the signal intensity of syntaxin4 in the permeabilized cells is weaker than or similar to that of β-actin (Fig 1B), the lower left graph reflects the expression amount of extracellular syntaxin4.

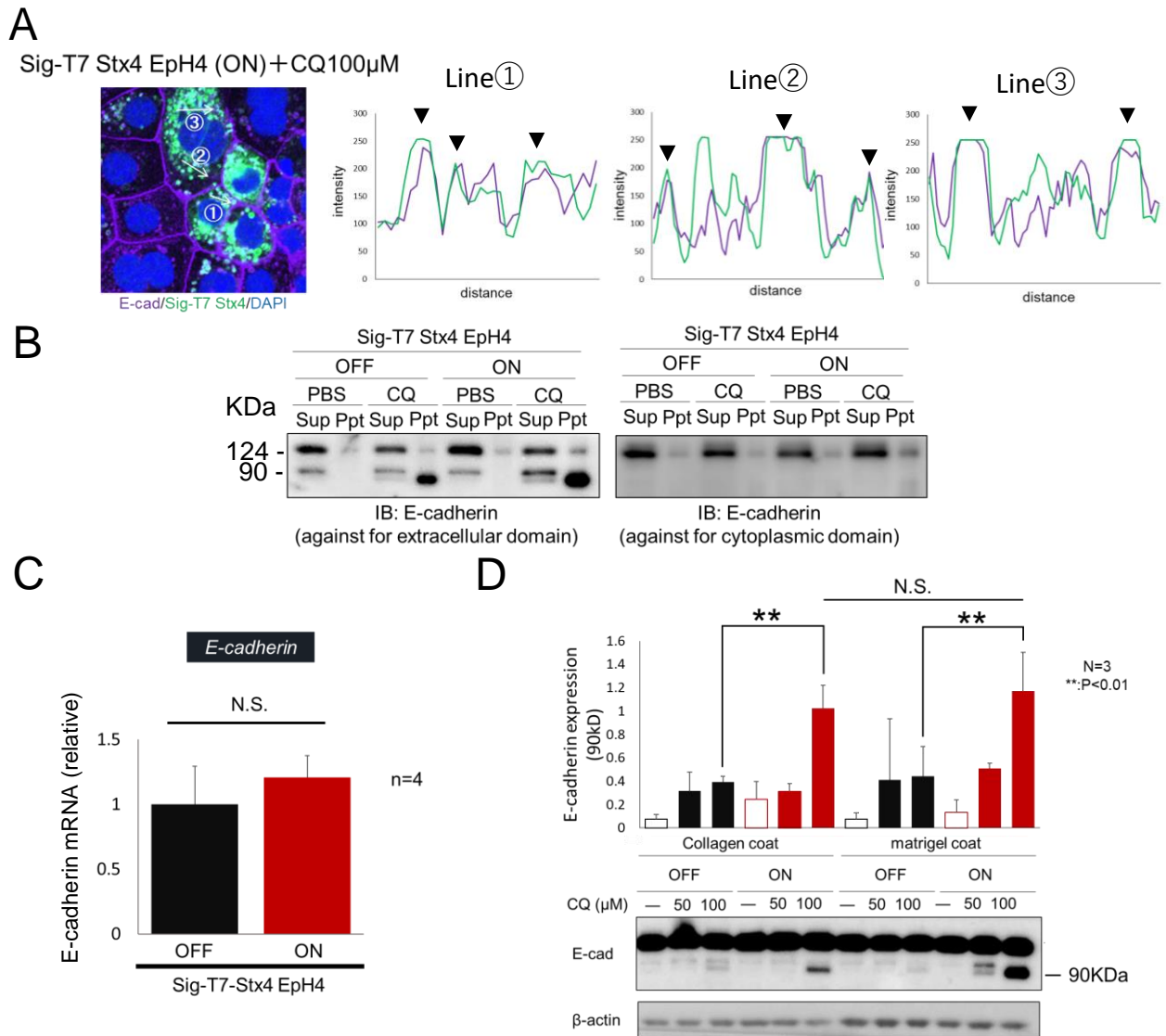




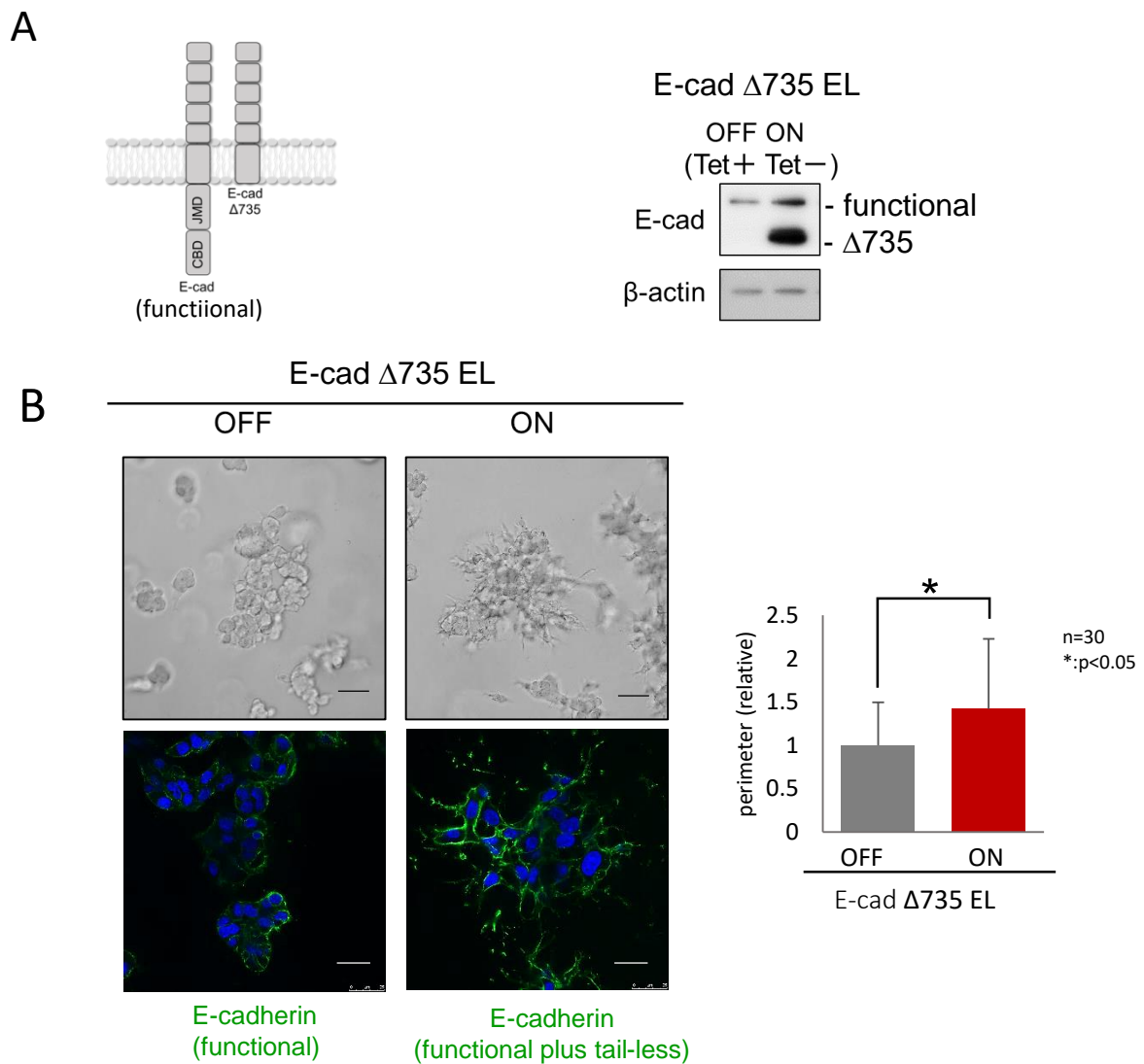
**Fig. S3.** Sig-T7 Stx4 EpH4 cell aggregates with extracellular syntaxin-4 (ON) were embedded in Matrigel or collagen I and compared the morphological appearance on day 5. In collagen gel Sig-T7 Stx4 EpH4 cells scattered/disseminated and never underwent luminal morphogenesis.



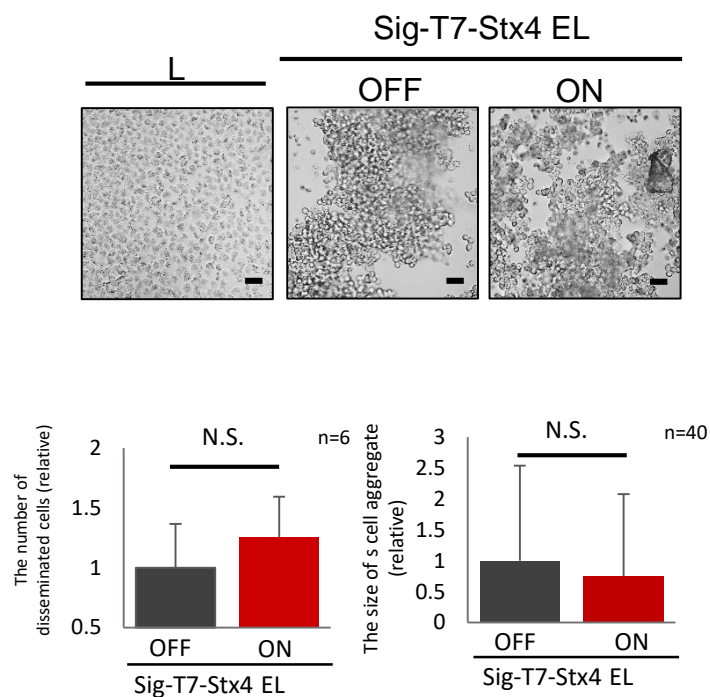
**Fig. S4.** Syntaxin4 binds to E-cadherin in EpH4 cells via its central and membrane proximal domain. Syntaxin4 fragments (r-F1:Met1-Glu110, r-F2:Ala111-Arg197, r-F3:Glu198-Lys272) tagged with 6X histidine residues were prepared, trapped to Ni-NTA agarose beads, and incubated with EpH4 cell lysate. Unbound and bound materials to the beads were collected and analyzed for E-cadherin by immunoblotting (upper). Equivalent amount of each fragment on the beads was apparent, as judged by Coomassie Brilliant Blue (CBB) staining (lower). The central domain (F2) and membrane proximal domain (F3) bound to E-cadherin expressed in EpH4 cells.



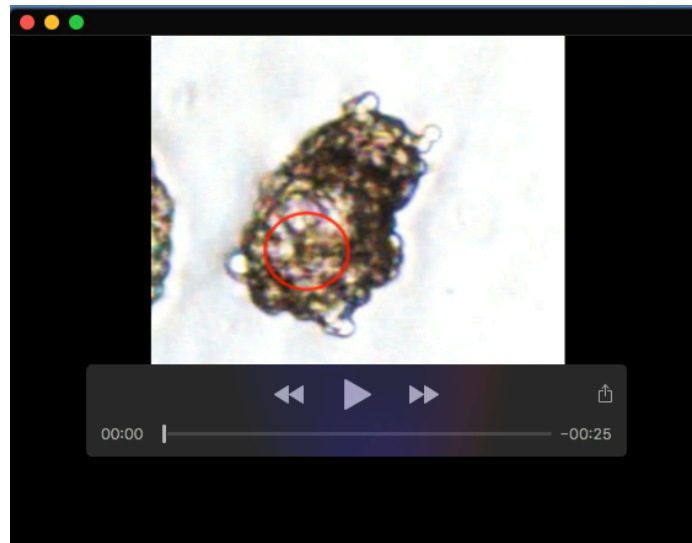
**Fig. S5.** A, Line scan analyses of E-cadherin (magenta) and sig-T7-Stx4 (green) in sig-T7-Stx4 EpH4 (ON) treated with CQ (same as a lower panel in Fig. 6E). Signal intensities of E-cadherin and sig-T7-Stx4 were analyzed along lines ①, ②, ③ using imageJ. Overlap of each maximum signal intensity shows colocalization of E-cadherin and sig-T7-Stx4 (triangles). B, The 90 kDa form of E-cadherin lacks cytoplasmic tail for cytoskeletal linkage. A monoclonal antibody against extracellular domain of E-cadherin (ECCD2) bound both the full length and the 90 kDa form of E-cadherin, whereas polyclonal antibodies against the cytoplasmic tail (Takara, Japan) failed to recognize the latter. C, Expression of extracellular syntaxin4 for 3 days did not affect the expression of E-cadherin mRNA in EpH4 cells.  $n=4$ . D, Signals from Matrigel did not affect the generation of 90 kDa E-cadherin. Sig-T7 Stx4 EpH4 cells on Matrigel or collagen I were treated with various amount of CQ, then the expression of E-cadherin was analyzed. These cells produced 90kDa E-cadherin in response to extracellular syntaxin4 even on Matrigel.  $N=3$ , \*\*,  $p<0.01$ .



**Fig. S6.** A, Left, a schematic image of full length (functional) and “tailless” E-cadherin-mutant (E-cad  $\Delta$ 735: Met1~Arg735). Right, EL cells with inducible expression of “tailless” E-cadherin-mutant (E-cad $\Delta$ 735 EL). EL cells were stably transfected with the PiggyBac-based tet-regulatable expression plasmid containing cDNA for Met1-Arg735 in *E-cadherin* (NCBI 12550). Upon removal of tetracycline (ON), these cells expressed “tailless” E-cadherin-mutant without affecting the amount of functional E-cadherin. B, Left, microscopy images and distribution of E-cadherin in E-cad $\Delta$ 735 EL cell aggregates embedded in Matrigel for three days. Bars, 50  $\mu$ m (upper) and 25  $\mu$ m (lower). Right, quantification of the perimeter of the cell aggregates. n= 30, \*, p< 0.05. Cell aggregates with only functional E-cadherin remained as cell clumps, whereas those additionally with E-cad $\Delta$ 735 were dissociated and scattered.



**Fig. S7.** Upper, light microscopy images of sig-T7-Stx4-EL cells with (ON) and without (OFF) extracellular expression of syntaxin4 in the cell dissociation assay. L cells that have no cadherins were completely dissociated by this treatment. Bars, 50 µm. Lower, relative number of dissociated single cells (left, n= 6), and the size of the undissociated cell aggregates (right, n= 40) after treatment with trypsin in the presence of Ca<sup>2+</sup>.



**Movie 1.** Sig-T7-Stx4 EpH4 aggregates were embedded in Matrigel and time-lapse images were acquired from 48 h of culture and ran for 120 h. Movie was constructed from expanded images from 99 h to 164 h when active cell movement was observed. Red circle indicates the inner cell populations in the aggregate.